doi:10.21608/esju.2025.359062.1070 Research Article
The Egyptian Statistical Journal (ESJ), 69 (1): 173-205

Homepage: https://esju.journals.ekb.eg/

The Egyptian Statistical Journal

Print ISSN 0542-1748– Online ISSN 2786-0086

Tangent Exponentiated Odd Log-Logistic Weibull Quantile Regression with Applications to Complete and Censored Data

Mohammed Hashim Bamba Mustapha [1], Jakperik Dioggban[2], Suleman Nasiru[3]

Received 19 February 2025; revised 19 May 2025; accepted 26 May 2025; Online June 2025

Keywords

Quantile regression; GAMLSS; Heteroscedasticity; Quantile residuals, Gaussian; Weibull distribution.

Abstract

A contemporary quantile regression model is formulated utilizing the tan exponentiated odd log-logistic Weibull distribution proposed in this study. The novel regression model is capable of modeling both complete and censored data, making it desirable for survival/reliability analysis. Through reparameterization of the probability density function of the tan exponentiated odd log-logistic Weibull distribution in terms of its quantile function, a suitable quantile regression framework is attained. The estimates of the parameters are attained using the maximum likelihood estimation technique. The findings of the Monte Carlo simulation studies conducted in the study affirm the accuracy of the model under varying levels of censoring and sample sizes. The utilities of the proposed quantile regression model are illustrated by applying it to model gastric cancer and rent datasets, demonstrating superior fit compared to competing models. This work extends the toolkit of quantile regression techniques by proposing a flexible model suitable for handling complete and censored outcomes effectively.

Mathematical Subject Classification: 62F10, 62G08

1. Introduction

Regression analysis has advanced considerably since the 20th century, moving beyond the traditional Gaussian (normal) framework (Prataviera et al., 2021). The evolution of regression analysis began with the linear model (LM) (Galton, 1886) through the generalized linear model (GLM) (Nelder and Wedderburn, 1972), generalized additive model (GAM) (Hastie and Tibshirani, 1986), and the generalized additive model for location, scale, and shape (GAMLSS) (Rigby and Stasinopoulos, 2005) demonstrating the growing trend and complexity ingrained in real-world data. LMs create standard models that predict a continuous response variable using a linear combination of predictor variables. Although LMs are widely applied across several fields to model real data, many phenomena are not usually in conformity with the assumptions of normality. This is usually due to the lack of symmetry in the distribution or the presence of heavy tails. Furthermore, LM typically assumes that the variability of errors is homogeneous. When this assumption is violated, it can adversely affect the efficiency of the estimators (Rodrigues et al., 2023a). The GLMs extend the LMs to accommodate responses that follow distributions other than the normal

✉ Corresponding author*: mhmustapha.stu@cktutas.edu.gh
[1,3]Department of Statistics and Actuarial Science, School of Mathematical Sciences,C. K. Tedam University of Technology and Applied Sciences, Navrongo, Ghana.
[2]Department of Biometry, School of Mathematical Sciences, C. K. Tedam University of Technology and Applied Sciences, Navrongo, Ghana

distribution. It provides a flexible modeling framework that makes it possible to handle various types of variables, such as binary, count, and continuous, by specifying an appropriate distribution and link function. The GAMs further generalize the GLMs by allowing the linear predictor to include smooth functions, potentially nonlinear functions of the predictor variables. This enables the model to capture complex, nonlinear relationships between predictors and response variables.

The most recent is the GAMLSS, which offers a thorough framework for modeling data with intricate features, including skewness, kurtosis, and heteroscedasticity. Since GAMLSS is a distribution-based approach to parametric and semiparametric regression analyses and an expanded version of GLM and GAM, it is more reliable and flexible. It enables the modeling of both linear and nonlinear effects of the covariates, allowing not only the estimation of the mean (location) but also the variance (scale), skewness, and kurtosis (shape) of the distribution (Stasinopoulos et al., 2017).

In a situation where the response variable involves outliers, highly skewed, bimodal, or multimodal, the conditional mean regression may yield misleading results. Unlike traditional mean regression, the quantile regression (QR) introduced by Koenker and Bassett (1978) is capable of capturing the heterogeneity effects of response variables (Stasinopoulos et al., 2017). The QR measures the varying impacts of the covariates by analyzing the conditional quantiles of the response variable, offering a thorough examination of the entire distribution of the outcome. For instance, in the presence of asymmetries and heavy tails, the sample median serves as a more accurate representation of the central tendency compared to the mean (Huang et al., 2017). Due to its flexibility and ability to provide insight into different quantiles and to capture complex relationships, the QR model has gained increasing recognition in modern applications. Some instances of these models for both bounded and unbounded responses include: the unit Weibull QR (Mazucheli et al., 2020), unit Birnbaum–Saunders QR (Mazucheli et al., 2021), arcsecant hyperbolic normal QR (Korkmaz et al., 2021), unit exponentiated Fréchet QR (Abubakari et al., 2022), Poisson-unit-Weibull QR (Muhammad et al., 2024), modified Kies Topp-Leone QR (Alghamdi et al., 2024), Unit Gamma/Gompertz QR (Mustapha et al., 2022), Vasicek QR (Mazucheli et al., 2022), arctan power QR (Nasiru et al., 2023), unit-Chen QR (Korkmaz et al., 2022), unit generalized half-normal QR (Mazucheli et al., 2023), unit Burr XII (Ribeiro et al., 2022), trigonometric QR (Nasiru and Chesneau, 2023), exponentiated odd log-logistic normal QR (Rodrigues et al., 2023c), generalized gamma QR (Noufaily and Jones, 2013), exponentiated odd log-logistic Weibull (EOLLW) QR (Rodrigues et al., 2023b), odd log-logistic Weibull QR (Rodrigues et al., 2022), Weibull QR (Sánchez et al., 2021), and Burr XII QR (de Araújo et al., 2022).

The traditional Weibull distribution, commonly used as a lifetime model for failure rates, only accommodates monotonic behaviors. It lacks the ability to represent bathtub-shaped and non-monotonic patterns, making it unsuitable for modeling complex lifetime data (Peng and Yan, 2014). To address these limitations, several extensions of the Weibull distribution have been introduced, allowing for greater flexibility by incorporating additional parameters and schemes notably: Log-beta Weibull (Ortega et al., 2013), three-parameter new extended Weibull (Peng and Yan, 2014), generalized flexible Weibull (Ahmad and Iqbal, 2017), log odd log-logistic Weibull (Cruz et al., 2016), Weibull extended Weibull (Cordeiro et al., 2023), Maxwell-Weibull (Ishaq and Abiodun, 2020), alpha logarithmic transformed Weibull (Nassar et al., 2018), exponentiated odd log-logistic Weibull (Rodrigues et al., 2023b), three-parameter modified Weibull (Ghazal, 2023), exponentiated modified Weibull extension (Sarhan and Apaloo, 2013), the exponentiated additive Weibull (Abd EL-Baset and Ghazal, 2020), log-normal modified Weibull (Shakhatreh et al., 2019), improved modified Weibull (Jiang et al., 2023), odd beta prime-Weibull (Suleiman et al., 2024) among others.

The exponentiated odd log-logistic (EOLL G) family (Alizadeh et al., 2020) with two shape parameters is capable of handling data with various skewness and tailed behaviors. The tangent-G (tan-G) family can capture intricate hazard shapes. These two families are blended to form a novel tangent exponentiated odd log-logistic (TEOLL) family (Souza et al., 2021). This integration exploits the complementary strengths of both families, offering greater modeling flexibility for complex hazard and tail behaviors. Thus, we propose a novel QR model based on a reparameterized tan exponentiated odd log-logistic Weibull (TEOLLW) distribution. The proposed model aims to enrich the statistical literature by offering a flexible framework for survival and reliability studies.

The rest of this study is structured as follows: Section 2 introduces the new distribution and some of its key features. Section 3 describes the TEOLLW QR model, parameter estimation, and quantile residual diagnostics. Section 4 conducts simulation analysis to examine the finite sample behavior of the maximum likelihood estimators. Section 5 offers real-life applications that use the proposed QR model and a residual analysis to evaluate the efficacy of the new model. The conclusions of the study are presented in Section 6.

2. Methodology

2.1 Tan Exponentiated Odd Log-Logistic Weibull Distribution

The TEOLL family is obtained by replacing the cumulative distribution function (CDF) and the probability density function (PDF) of the baseline distribution in the tan-G family with the CDF and PDF of the EOLL-G family. Suppose Z is a continuous random variable that follows the CDF of the exponentiated odd log-logistic family, then the CDF of the newly generated TEOLL family is given by

$$G(z) = tan\left[\Lambda_{z;\Psi}\right], z \in R, \theta > 0, \lambda > 0, \tag{1}$$

where $\Lambda_{z;\Psi} = \tan\left[\frac{\pi[D(z;\psi)]^{\theta\lambda}}{4\{[D(z;\psi)]^{\theta} + [1-D(z;\psi)]^{\theta}\}^{\lambda}}\right]$, θ and λ are shapes parameters, and π is a constant approximately equal to $\frac{22}{7}$.

The corresponding PDF, survival function (SF), and hazard rate function (HRF) are respectively given by

$$g(z) = \frac{\pi\theta\lambda d(z;\psi)[D(z;\psi)]^{\theta\lambda-1}[1-D(z;\psi)]^{\theta-1}}{4\{[D(z;\psi)]^{\theta} + [1-D(z;\psi)]^{\theta}\}^{\lambda+1}} sec^2\left[\Lambda_{z;\Psi}\right],\ z \in R, \tag{2}$$

$$H(z) = 1 - tan\left[\Lambda_{z;\Psi}\right], z \in R, \tag{3}$$

and

$$H(z) = \frac{\pi\theta\lambda d(z;\psi)[D(z;\psi)]^{\theta\lambda-1}[1-D(z;\psi)]^{\theta-1} sec^2\left[\Lambda_{z;\Psi}\right]}{4\{[D(z;\psi)]^{\theta} + [1-D(z;\psi)]^{\theta}\}^{\lambda+1}\left\{1 - tan\left[\Lambda_{z;\Psi}\right]\right\}}, z \in R. \tag{4}$$

The study adopts the traditional Weibull distribution with two parameters as the baseline distribution. Given the CDF, $D(z)=1-\exp\left[-(z/\rho)^{\sigma}\right]$ of the Weibull distribution and its corresponding PDF, $d(z)=(\sigma/\rho^{\sigma})z^{\sigma-1}\exp\left[-(z/\rho)^{\sigma}\right]$, where $z>0$, $\rho>0$ and $\sigma>0$. Let Z follow the TEOLLW distribution, the CDF of the new distribution is given by

$$G(z)=\tan\left\{\frac{\pi(1-m)^{\theta\lambda}}{4\left[m^{\theta}+(1-m)^{\theta}\right]^{\lambda}}\right\},\quad z>0, \tag{5}$$

where $m=e^{-\left(\frac{z}{\rho}\right)^{\sigma}}$, $\lambda>0$, $\sigma>0$ and $\theta>0$ are shape parameters and $\rho>0$ is a scale parameter. The corresponding PDF $g(z)$ is obtained by differentiating Equation (5) with respect to z and is given by

$$g(z)=\frac{\theta\lambda\sigma\pi z^{\sigma-1}m^{\theta}(1-m)^{\theta\lambda-1}}{4\rho^{\sigma}\left[m^{\theta}+(1-m)^{\theta}\right]^{\lambda+1}}\sec^{2}\left[\frac{\pi(1-m)^{\theta\lambda}}{4\left[m^{\theta}+(1-m)^{\theta}\right]^{\lambda}}\right],\ z>0. \tag{6}$$

The associated SF of the TEOLLW distribution is given by

$$S(z)=1-\tan\left|\frac{\pi(1-m)^{\theta\lambda}}{4\left[m^{\theta}+(1-m)^{\theta}\right]^{\lambda}}\right|,\quad z>0, \tag{7}$$

The HRF which is the ratio of PDF to SF is also given by

$$H(z)=\frac{\theta\lambda\sigma\pi z^{\sigma-1}m^{\theta}(1-m)^{\theta\lambda-1}\left[m^{\theta}+(1-m)^{\theta}\right]^{-(\lambda+1)}}{4\rho^{\sigma}\left\{1-\tan\left[\frac{\pi(1-m)^{\theta\lambda}}{4\left[m^{\theta}+(1-m)^{\theta}\right]^{\lambda}}\right]\right\}}\sec^{2}\left[\frac{\pi(1-m)^{\theta\lambda}}{4\left[m^{\theta}+(1-m)^{\theta}\right]^{\lambda}}\right],z>0. \tag{8}$$

The plots of the PDF and HRF of the TEOLLW distribution for different combinations of parameter values are shown in Figure 1. The PDF exhibits left-skewed, right-skewed, decreasing, and approximately symmetric shapes. The HRF displays bathtub, increasing and decreasing failure rate shapes.

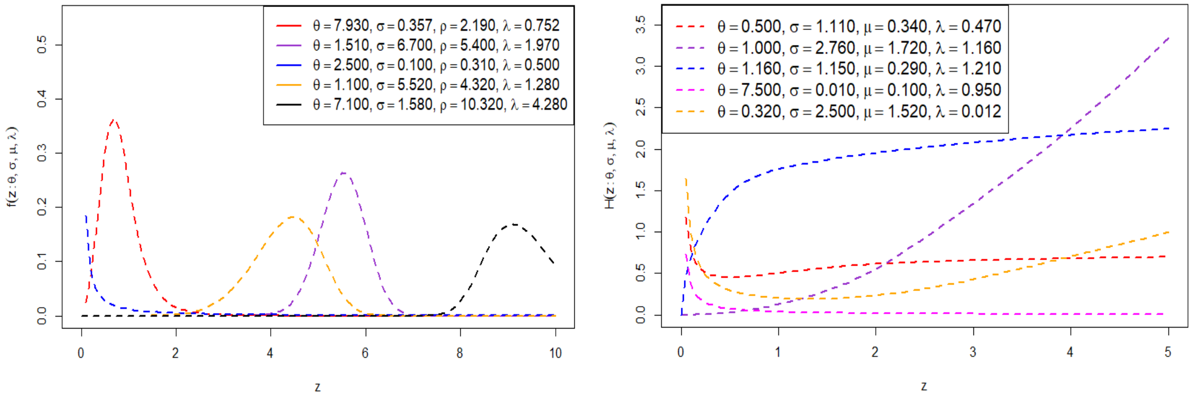

Figure 1. TEOLLW distribution plots for the PDF and HRF

The corresponding quantile function is given by

$$Q(u;\rho,\sigma,\theta,\lambda)=\rho\left\{-\log\left[\frac{\left(1-\left(\frac{4\arctan(u)}{\pi}\right)^{\frac{1}{\lambda}}\right)^{\frac{1}{\theta}}}{\left(\frac{4\arctan(u)}{\pi}\right)^{\frac{1}{\theta\lambda}}+\left(1-\left(\frac{4\arctan(u)}{\pi}\right)^{\frac{1}{\lambda}}\right)^{\frac{1}{\theta}}}\right]\right\}^{\frac{1}{\sigma}},u\in(0,1). \quad (9)$$

3. Results

3.1 TEOLLW QR Model

The GAMLSS package (Stasinopoulos et al., 2017) is available in the R software and was used to implement the TEOLLW QR model. The PDF in Equation (6) is reparameterized in terms of the quantile function of the TEOLLW distribution to develop the new QR. Letting $\mu=Q(u;\rho,\sigma,\theta,\lambda)$ and making ρ the subject yields

$$\rho=\mu\left\{-\log\left[\frac{(1-\Theta)^{\frac{1}{\theta}}}{\Theta^{\frac{1}{\theta}}+(1-\Theta)^{\frac{1}{\theta}}}\right]\right\}^{-\frac{1}{\sigma}},\tau\in(0,1), \quad (10)$$

where $\Theta=\left(\frac{4\arctan(\tau)}{\pi}\right)^{\frac{1}{\lambda}}$ and $\mu>0$ is the quantile parameter.

By substituting Equation (10) into Equation (6), the reparameterized PDF of Z is given by

$$g(z)=\frac{\theta\lambda\sigma\Upsilon\Psi z^{\sigma-1}\sec^2\left\{\frac{\pi[1-\Psi]^{\theta\lambda}}{4\left\{\Psi^{\theta}+(1-\Psi)^{\theta}\right\}^{\lambda}}\right\}}{4\mu^{\sigma}[1-\Psi]^{1-\theta\lambda}\left\{\Psi^{\theta}+(1-\Psi)^{\theta}\right\}^{\lambda+1}},\qquad z>0, \quad (11)$$

where $\Upsilon(\tau,\theta,\lambda) = -\log\left[\dfrac{(1-\Theta)^{\frac{1}{\theta}}}{\Theta^{\frac{1}{\theta}}+(1-\Theta)^{\frac{1}{\theta}}}\right]$, $\Psi = e^{-\Upsilon\left(\frac{z}{\mu}\right)^{\sigma}}$, $\lambda>0,\ \theta>0,\ \sigma>0,\ \mu>0$ and $\tau\in(0,\ 1)$.

The following submodels can be generated from the TEOLLW distribution;

- The tan odd log-logistic Weibull (TOLLW) distribution when $\lambda=1$,
- and tan Weibull (TW) when $\lambda=\theta=1$.

Suppose $z_1,\ z_2,\ ...,\ z_n$ are random samples from the TEOLLW distribution with PDF given in Equation (11) with varying scale parameter, μ_i and shape parameter, σ_i and also $t_i^T = (t_{i1},\ ...,\ t_{iq})$ is a vectors of fixed covariates for the i^{th} observation. Consider two systematic components;

$$\mu_i(\tau)=e^{t_i^T\phi_1(\tau)} \qquad \text{and} \qquad \sigma_i(\tau)=e^{t_i^T\phi_2(\tau)}, \tag{12}$$

for $i=1,\ 2,\ ...,\ n$. Again $\phi_1(\tau)=(\phi_{10},\ \phi_{11},\ ...,\ \phi_{1q})^T$ and $\phi_2(\tau)=(\phi_{20},\ \phi_{21},\ ...,\ \phi_{2q})T$ are unknown vectors of parameters of dimension q.

The TOLLW QR obtained by inserting equation (12) into (11) is given by

$$g(z)=\frac{\theta\lambda\sigma_i(\tau)z^{\sigma_i(\tau)-1}\Upsilon\Omega_i\sec^2\left\{\dfrac{\pi[1-\Omega_i]^{\theta\lambda}}{4\left\{\Omega_i^{\theta}+(1-\Omega_i)^{\theta}\right\}^{\lambda}}\right\}}{4(\mu_i)^{\sigma_i(\tau)}[1-\Omega_i]^{1-\theta\lambda}\left\{\Omega_i^{\theta}+(1-\Omega_i)^{\theta}\right\}^{\lambda+1}}, \qquad z>0, \tag{13}$$

where $\Omega_i = e^{-\Upsilon\left(\frac{z}{\mu_i}\right)^{\sigma}}$.

3.2 Maximum Likelihood Estimation

The study employed the maximum likelihood estimation (MLE) technique to find the parameter estimates of the TEOLLWQR model. When dealing with complete data, the total log-likelihood function for the parameter vector, $\xi=(\phi_1^T(\tau),\phi_2^T(\tau),\theta,\lambda)^T$ is given by

$$\ell(\xi)=n\log(\theta\lambda\Upsilon)+\sum_{i=1}^{n}[\Omega_i\sigma_i(\tau)]+\sum_{i=1}^{n}\left\{\sec^2\left[\frac{\pi[1-\Omega_i]^{\theta\lambda}}{4\left\{\Omega_i^{\theta}+(1-\Omega_i)^{\theta}\right\}^{\lambda}}\right]\right\}$$
$$-4\sum_{i=1}^{n}[\mu_i^{\sigma_i(\tau)}]+(\theta\lambda-1)\sum_{i=1}^{n}(1-\Omega_i)-\sum_{i=1}^{n}[\Omega_i^{\theta}+(1-\Omega_i)^{\theta}]. \tag{14}$$

For censored data, suppose that Z_i represent the lifetime and V_i represent censoring time for the i^{th} individual. The observation time is given by $z_i = \min\{Z_i, V_i\}$ and the total log-likelihood is

$$\ell(\xi) = q\log(\theta\lambda\Upsilon) + \sum_{i\in H}[\Omega_i\sigma_i(\tau)] + \sum_{i\in H}\left\{\sec^2\left[\frac{\pi[1-\Omega_i]^{\theta\lambda}}{4\left\{\Omega_i^{\theta}+(1-\Omega_i)^{\theta}\right\}^{\lambda}}\right]\right\}$$
$$-4\sum_{i\in H}[\mu_i^{\sigma_i(\tau)}] + (\theta\lambda-1)\sum_{i\in H}(1-\Omega_i) - \sum_{i\in H}[\Omega_i^{\theta}+(1-\Omega_i)^{\theta}]$$
$$+\sum_{i\in V}\left\{1-\tan\left[\frac{\pi[1-\Omega_i]^{\theta\lambda}}{4\left\{\Omega_i^{\theta}+(1-\Omega_i)^{\theta}\right\}^{\lambda}}\right]\right\}, \tag{15}$$

where q is the number of uncensored observations, H is the set of units with lifetime and V is units with censored time.

3.3 Randomized Quantile Residuals

The validation of the model is done by performing residual analysis. The randomized quantile residuals introduced by Dunn and Smyth (1996) is employed in this study. The randomized quantile residuals are given by

$$\hat{r}_i = \phi^{-1}(\hat{\kappa}_i), \tag{16}$$

where $\hat{\kappa}_i = G(z;\widehat{\Omega})$ is the estimated CDF and $\phi^{-1}(\bullet)$ is the inverse of the standard normal CDF. When the fitted model is valid for the dataset, the residuals are normally distributed with zero mean and unit variance.

4. Simulation Study

In this section, Monte Carlo simulations are conducted to investigate the behavior of the maximum likelihood estimates (MLEs). Random observations of sample sizes, $n = 25,\ 100,\ 150,\ 200$ and 250 are generated from the reparameterized TEOLLW distribution and four censoring percentages, CP = 0%, 30%, 50% and 80% are incorporated to cover scenarios from complete data to highly censored datasets. Three quantiles $\tau = 0.25,\ 0.50$ and 0.75 are considered. For each quantile level, a distinct set of true parameter values is specified:

- Set 1: $\{-2.5,\ 0.5, -1.0,\ 0.3, -0.5,\ 0.4\}$ for 0.25 quantile,
- Set 2: $\{-0.4,\ 0.6, -0.5,\ 0.9,\ 0.5,\ 0.8\}$ for 0.50 quantile, and
- Set 3: $\{-0.1,\ 0.3, -0.3,\ 0.4, -0.2,\ 0.2\}$ for 0.75 quantile.

The process is repeated $1{,}000$ times for each combination of quantile level, sample size, and censoring percentage. The regression structure employed in the simulation experiments is as follows;

$$M = \begin{cases} \mu_i = \exp[\phi_{10} + \phi_{11} t_{i1}] \\ \sigma_i = \exp[\phi_{20} + \phi_{21} t_{i1}] \\ \theta_i = \exp[\phi_{30}] \\ \lambda_i = \exp[\phi_{40}] \end{cases}$$

where t_{1i} is an explanatory variable drawn from a uniform distribution within the range $(0,\ 1)$. The performance of the MLEs is assessed by calculating average estimates (AEs), mean square errors (MSEs), root mean square errors (RMSEs), and 95% confidence intervals (CIs). The findings presented in Tables 1, 2, and 3 revealed that as n increases, the AEs approach their true values, MSEs and RMSEs decrease, and CIs become tighter, confirming the consistency of the estimators. Also, as the CP increases, the AEs become more biased, and the MSEs, RMSEs, and CIs increase, indicating that the MLE finds it more difficult to consistently obtain the true parameter values when censoring increases.

Table 1a. AE, MSE, RMSE, and 95% CI for MLEs of TEOLLW QR model at $\tau = 0.25$ and CP = (0% and 30%)

n	Parameter	CP=0					CP=0.30				
		AE	MSE	RMSE	LCL	UCL	AE	MSE	RMSE	LCL	UCL
25	ω_{10}	-4.1500	6.0582	2.4613	-7.8373	-0.5951	-4.2010	6.3075	2.5115	-7.8713	-0.6526
	ω_{11}	0.8811	9.1678	3.0278	-4.9483	7.0217	0.7915	10.2590	3.2030	-5.6979	6.8665
	ω_{20}	-1.0376	1.8099	1.3453	-4.4771	1.2997	-1.4762	5.4537	2.3353	-6.8660	1.9607
	ω_{21}	0.2910	0.5797	0.7614	-0.9969	1.8400	0.2886	1.0800	1.0392	-1.8359	2.3095
	ω_{30}	-0.2126	1.4209	1.1920	-1.6063	2.9913	0.1601	4.6984	2.1676	-2.1558	5.8609
	ω_{40}	0.6626	1.6848	1.2980	-1.4180	3.6274	1.2249	4.4052	2.0989	-1.1913	5.6895
100	ω_{10}	-4.2753	3.8210	1.9547	-5.8103	-2.5952	-4.3459	4.1649	2.0408	-6.1166	-2.6447
	ω_{11}	1.0007	2.0108	1.4180	-1.8083	3.4025	1.0737	2.2755	1.5085	-1.8102	3.7414
	ω_{20}	-1.2690	0.1882	0.4339	-1.8829	-0.5671	-1.5936	2.1761	1.4752	-6.5691	0.8866
	ω_{21}	0.3135	0.0778	0.2790	-0.2270	0.8855	0.3302	0.1465	0.3827	-0.3990	1.0869
	ω_{30}	-0.1411	0.3707	0.6089	-1.1255	0.9430	-0.0354	2.3512	1.5334	-1.4624	5.6401
	ω_{40}	0.5574	0.4259	0.6526	-0.6766	1.6664	0.8846	1.2853	1.1337	-0.8167	2.7609
150	ω_{10}	-4.2558	3.5168	1.8753	-5.5671	-2.9475	-4.2813	3.6607	1.9133	-5.6876	-2.8911
	ω_{11}	0.9793	1.3356	1.1557	-1.1482	2.9545	0.9770	1.4651	1.2104	-1.2563	3.1572
	ω_{20}	-1.3141	0.1688	0.4109	-1.7805	-0.8052	-1.5430	1.5639	1.2506	-4.1609	0.4504
	ω_{21}	0.3137	0.0524	0.2289	-0.1501	0.7620	0.3192	0.0997	0.3157	-0.2690	0.9292
	ω_{30}	-0.3310	0.2118	0.4602	-1.2837	0.3916	-0.1356	1.7580	1.3259	-1.5048	3.6846
	ω_{40}	0.8147	0.5745	0.7579	-0.3225	1.9604	0.8951	0.9643	0.9820	-0.6629	2.2090
200	ω_{10}	-4.2725	3.4996	1.8707	-5.5414	-3.1877	-4.2909	3.5940	1.8958	-5.5747	-3.1820
	ω_{11}	0.9891	1.1634	1.0786	-0.6290	2.9671	0.9939	1.2128	1.1013	-0.7058	3.0485
	ω_{20}	-1.2932	0.1536	0.3919	-1.7227	-0.7951	-1.5992	1.7489	1.3225	-6.5242	-0.0454
	ω_{21}	0.3034	0.0398	0.1994	-0.0506	0.6926	0.3074	0.0759	0.2756	-0.2516	0.8101
	ω_{30}	-0.2821	0.2350	0.4848	-1.2396	0.4555	-0.1221	1.9759	1.4057	-1.2913	5.5571
	ω_{40}	0.7281	0.4760	0.6900	-0.3259	1.8530	0.9197	0.8851	0.9408	-0.6942	2.0735

n	Parameter	CP=0					CP=0.30				
		AE	MSE	RMSE	LCL	UCL	AE	MSE	RMSE	LCL	UCL
250	ω_{10}	-4.2475	3.3462	1.8292	-5.2815	-3.1618	-4.2738	3.4729	1.8636	-5.3976	-3.1339
	ω_{11}	0.9114	0.9126	0.9553	-0.7715	2.5589	0.9286	1.0148	1.0074	-0.9125	2.8277
	ω_{20}	-1.2630	0.1094	0.3308	-1.6243	-0.8575	-1.7439	2.4131	1.5534	-7.1292	0.0247
	ω_{21}	0.2939	0.0324	0.1801	-0.0344	0.6439	0.3003	0.0660	0.2570	-0.2566	0.8035
	ω_{30}	-0.1572	0.2739	0.5233	-1.0650	0.7137	0.3142	3.1355	1.7707	-1.1064	6.3566
	ω_{40}	0.5493	0.3422	0.5849	-0.3985	1.6837	0.5593	0.6046	0.7776	-0.6986	1.8242

Table 1b. AE, MSE, RMSE and 95% CI for MLEs of TEOLLW QR model at $\tau = 0.25$ and CP = (50% and 80%)

n	Parameter	CP=0.50					CP=0.80				
		AE	MSE	RMSE	LCL	UCL	AE	MSE	RMSE	LCL	UCL
25	ω_{10}	-4.2441	6.9054	2.6278	-8.4526	-0.9198	-4.0666	12.0605	3.4728	-8.0585	4.3600
	ω_{11}	0.8626	10.8395	3.2923	-5.4115	7.3610	0.5629	29.7483	5.4542	-12.9508	8.8387
	ω_{20}	-1.4972	7.0393	2.6532	-6.7704	2.2211	-0.7408	5.8901	2.4270	-5.4631	2.3600
	ω_{21}	0.2953	1.6801	1.2962	-2.3283	2.8735	0.2988	4.6819	2.1638	-4.4636	3.7168
	ω_{30}	0.2719	6.3433	2.5186	-2.5190	5.5179	-0.5451	6.6124	2.5714	-3.2528	4.5302
	ω_{40}	1.3796	5.3805	2.3196	-1.2761	5.5176	1.3122	5.2392	2.2889	-2.4733	4.9470
100	ω_{10}	-4.3643	4.3137	2.0769	-6.1675	-2.6778	-4.3639	4.8137	2.1940	-6.4979	-1.8573
	ω_{11}	1.0612	2.4440	1.5633	-1.8074	3.7469	1.0601	5.2182	2.2843	-2.4203	6.1524
	ω_{20}	-1.7496	3.9010	1.9751	-6.7818	1.0335	-0.9244	3.8990	1.9746	-5.5721	1.6621
	ω_{21}	0.3354	0.2569	0.5068	-0.6156	1.3083	0.3170	0.7537	0.8682	-1.3566	1.9435
	ω_{30}	0.2977	4.1504	2.0373	-1.8676	5.5799	-0.2345	4.8469	2.2016	-2.8825	3.9742
	ω_{40}	0.8910	2.2948	1.5149	-1.0142	4.6407	0.7538	3.0449	1.7450	-2.3535	4.7201
150	ω_{10}	-4.3072	3.7923	1.9474	-5.7161	-2.8816	-4.2837	4.3247	2.0796	-6.1980	-1.9528
	ω_{11}	0.9870	1.5490	1.2446	-1.1896	3.2717	0.9740	4.4795	2.1165	-2.4613	5.9842
	ω_{20}	-1.6572	3.0996	1.7606	-6.1460	0.9917	-1.0930	3.5987	1.8970	-5.6714	1.3903
	ω_{21}	0.3360	0.1545	0.3930	-0.5037	1.0797	0.3569	0.5481	0.7404	-1.0868	1.8418

n	Parameter	CP=0.50					CP=0.80				
		AE	MSE	RMSE	LCL	UCL	AE	MSE	RMSE	LCL	UCL
	ω_{30}	0.3553	3.5641	1.8879	-1.6988	5.1113	-0.0101	4.8639	2.2054	-2.7539	4.0774
	ω_{40}	0.5461	1.5434	1.2424	-1.2817	3.0226	0.5486	2.9783	1.7258	-2.4798	5.0813
200	ω_{10}	-4.3062	3.6799	1.9183	-5.7379	-3.1864	-4.3517	4.2162	2.0533	-6.0391	-2.5141
	ω_{11}	0.9973	1.2779	1.1304	-0.7650	3.1934	1.0544	3.1942	1.7872	-1.8361	4.9806
	ω_{20}	-1.4527	2.3365	1.5286	-6.0906	0.8637	-1.0093	3.4740	1.8639	-5.6292	1.4344
	ω_{21}	0.3146	0.1185	0.3442	-0.3786	0.9625	0.3158	0.3843	0.6199	-0.9169	1.4881
	ω_{30}	0.0750	2.4904	1.5781	-1.6839	4.9252	-0.1090	4.5090	2.1234	-2.7000	4.1349
	ω_{40}	0.5597	0.9292	0.9640	-0.8919	2.5527	0.4643	2.1513	1.4667	-2.3393	4.1756
250	ω_{10}	-4.2825	3.5270	1.8780	-5.3547	-3.0758	-4.3372	4.0137	2.0034	-5.7457	-2.7885
	ω_{11}	0.9191	1.0503	1.0249	-1.1104	2.7522	1.0143	2.4782	1.5742	-1.5111	4.1735
	ω_{20}	-1.4203	1.7587	1.3262	-3.8173	0.8953	-0.9693	2.6133	1.6166	-5.3066	1.2577
	ω_{21}	0.3157	0.1038	0.3221	-0.3838	0.9374	0.3002	0.2825	0.5315	-0.8331	1.2839
	ω_{30}	-0.2506	1.6061	1.2673	-1.7193	2.7201	-0.1410	3.8256	1.9559	-2.5849	3.8392
	ω_{40}	0.8934	1.1198	1.0582	-0.7379	2.4817	0.3849	1.8758	1.3696	-2.2884	3.9260

Table 2a. AE, MSE, RMSE and 95% CI for MLEs of TEOLLW QR model at $\tau = 0.50$ and CP = (0% and 30%)

n	Parameter	CP=0					CP=0.30				
		AE	MSE	RMSE	LCL	UCL	AE	MSE	RMSE	LCL	UCL
25	ω_{10}	-1.1275	1.0085	1.0043	-2.5895	0.1633	-1.1707	1.1698	1.0816	-2.7115	0.2327
	ω_{11}	1.0042	1.1033	1.0504	-0.8787	2.9745	1.0504	1.5040	1.2264	-1.1396	3.2504
	ω_{20}	-0.5775	1.6922	1.3008	-2.9316	1.7515	-1.3119	5.7346	2.3947	-6.7346	2.1625
	ω_{21}	0.9305	0.5653	0.7518	-0.3612	2.6396	0.9702	1.0066	1.0033	-0.9587	3.1466
	ω_{30}	-0.2362	1.9278	1.3885	-1.6100	2.8578	0.4229	5.1325	2.2655	-1.9226	6.5108
	ω_{40}	0.6996	1.9104	1.3822	-1.3765	4.1231	1.0474	3.3091	1.8191	-1.3180	5.4890
100	ω_{10}	-1.1867	0.7155	0.8459	-1.7877	-0.5709	-1.2121	0.7636	0.8738	-1.8242	-0.6203
	ω_{11}	1.0707	0.4078	0.6386	0.2022	1.8623	1.0937	0.4472	0.6687	0.2014	2.0068
	ω_{20}	-0.7534	0.1999	0.4471	-1.4479	0.0315	-1.1405	1.9693	1.4033	-6.3136	0.2700
	ω_{21}	0.9168	0.0775	0.2784	0.3862	1.4827	0.9373	0.0981	0.3131	0.3249	1.5859
	ω_{30}	-0.0319	0.5205	0.7215	-0.8945	1.2180	0.3725	2.2036	1.4845	-0.8192	6.5231
	ω_{40}	0.4105	0.6238	0.7898	-0.8839	1.6218	0.3972	0.9184	0.9583	-1.1098	1.9738
150	ω_{10}	-1.1758	0.6556	0.8097	-1.6592	-0.7391	-1.1840	0.6741	0.8210	-1.7074	-0.7023
	ω_{11}	1.0564	0.3119	0.5585	0.4515	1.6878	1.0573	0.3234	0.5686	0.3845	1.7434
	ω_{20}	-0.8457	0.2003	0.4475	-1.3727	-0.2874	-0.9191	0.3052	0.5525	-1.5433	-0.2261
	ω_{21}	0.9125	0.0522	0.2284	0.4461	1.3586	0.9336	0.0673	0.2594	0.4498	1.4758
	ω_{30}	-0.4386	1.0771	1.0378	-1.4480	0.0873	-0.4809	1.2086	1.0994	-1.5326	0.1045
	ω_{40}	0.9625	0.4671	0.6834	-0.2504	2.1307	1.0977	0.5815	0.7626	-0.2896	2.3419
200	ω_{10}	-1.1898	0.6782	0.8235	-1.6825	-0.7693	-1.1958	0.6897	0.8305	-1.6985	-0.7704
	ω_{11}	1.0708	0.3275	0.5723	0.4829	1.7599	1.0760	0.3297	0.5742	0.4937	1.7438
	ω_{20}	-0.8386	0.2021	0.4495	-1.4261	-0.2960	-0.9143	0.2880	0.5367	-1.5822	-0.3096
	ω_{21}	0.9021	0.0416	0.2040	0.5395	1.2974	0.9225	0.0548	0.2341	0.4687	1.3635
	ω_{30}	-0.4464	1.1431	1.0692	-1.5733	0.2505	-0.5402	1.2995	1.1400	-1.6570	0.0797
	ω_{40}	0.9214	0.5701	0.7550	-0.3128	2.4063	1.1343	0.6388	0.7993	-0.1731	2.4533

n	Parameter	CP=0					CP=0.30				
		AE	MSE	RMSE	LCL	UCL	AE	MSE	RMSE	LCL	UCL
250	ω_{10}	-1.1689	0.6321	0.7950	-1.5912	-0.8011	-1.1815	0.6574	0.8108	-1.6160	-0.8077
	ω_{11}	1.0395	0.2774	0.5266	0.4696	1.5819	1.0453	0.2959	0.5440	0.4571	1.6722
	ω_{20}	-0.8111	0.1642	0.4052	-1.3122	-0.3408	-0.9147	0.3404	0.5835	-1.6378	-0.3108
	ω_{21}	0.8873	0.0341	0.1846	0.5241	1.2491	0.9062	0.0426	0.2063	0.5272	1.3231
	ω_{30}	-0.3680	1.0248	1.0123	-1.5881	0.3567	-0.4263	1.3237	1.1505	-1.7282	0.6625
	ω_{40}	0.7908	0.5344	0.7310	-0.4236	2.1653	0.9570	0.7549	0.8689	-0.4902	2.6430

Table 2b. AE, MSE, RMSE and 95% CI for MLEs of TEOLLW QR model at $\tau = 0.50$ and CP = (50% and 80%)

n	Parameter	CP=0.50					CP=0.80				
		AE	MSE	RMSE	LCL	UCL	AE	MSE	RMSE	LCL	UCL
25	ω_{10}	-1.2154	1.5140	1.2305	-3.0242	0.7441	-1.5255	4.3828	2.0935	-3.9871	2.7673
	ω_{11}	1.1386	3.0052	1.7336	-1.7431	4.5135	1.4205	14.2008	3.7684	-3.5647	8.3998
	ω_{20}	-1.2784	6.7846	2.6047	-6.7163	2.4235	-1.3209	3.8286	1.9567	-4.3725	2.1161
	ω_{21}	0.9647	1.5164	1.2314	-1.4800	3.1582	0.8113	3.2817	1.8115	-2.5898	4.6302
	ω_{30}	0.4829	5.7870	2.4056	-2.3606	6.0530	-0.5361	5.1472	2.2688	-2.6969	5.1646
	ω_{40}	1.2250	4.0388	2.0097	-1.3897	5.7225	3.3999	29.1298	5.3972	-5.5175	13.7905
100	ω_{10}	-1.2278	0.8485	0.9212	-2.0203	-0.4599	-1.3618	1.7600	1.3267	-2.9112	0.9928
	ω_{11}	1.1125	0.6453	0.8033	-0.0564	2.3355	1.4429	5.5249	2.3505	-2.0470	6.2950
	ω_{20}	-1.2479	2.7036	1.6443	-6.3420	1.2718	-1.4300	3.8493	1.9620	-5.9697	1.5323
	ω_{21}	0.9369	0.2188	0.4678	0.0444	1.8461	0.9492	1.1886	1.0902	-0.9684	3.1479
	ω_{30}	0.3213	2.4394	1.5619	-1.3594	5.7812	-0.4394	4.5053	2.1226	-2.4819	5.3418
	ω_{40}	0.7907	1.8675	1.3666	-1.5571	3.8852	2.3388	10.2848	3.2070	-1.0557	9.7123
150	ω_{10}	-1.1815	0.7006	0.8370	-1.7395	-0.5797	-1.2831	1.2732	1.1284	-2.4227	0.3632
	ω_{11}	1.0444	0.4151	0.6443	0.1514	1.9931	1.2992	3.2001	1.7889	-1.1436	5.0614
	ω_{20}	-1.3074	3.1774	1.7825	-6.5835	1.0346	-1.2825	3.7253	1.9301	-6.0475	1.5977
	ω_{21}	0.9493	0.1601	0.4001	0.2217	1.6860	0.9810	0.8502	0.9221	-0.5968	2.6842

n	Parameter	CP=0.50					CP=0.80				
		AE	**MSE**	**RMSE**	**LCL**	**UCL**	**AE**	**MSE**	**RMSE**	**LCL**	**UCL**
	ω_{30}	0.3535	3.0570	1.7484	-1.3525	6.1595	0.0312	4.3882	2.0948	-2.3684	5.9973
	ω_{40}	0.6459	1.0017	1.0009	-0.8884	2.5829	1.2892	5.0785	2.2535	-3.4142	5.5153
200	ω_{10}	-1.1929	0.7008	0.8372	-1.7640	-0.7150	-1.2139	1.0884	1.0433	-2.3086	0.4138
	ω_{11}	1.0767	0.3981	0.6309	0.3496	1.9467	1.3149	2.4468	1.5642	-0.9127	4.6143
	ω_{20}	-0.9483	0.9336	0.9662	-2.0226	1.0294	-1.8980	5.1749	2.2748	-6.4572	0.8450
	ω_{21}	0.9303	0.1169	0.3418	0.1942	1.6007	0.8919	0.4640	0.6812	-0.4079	2.2132
	ω_{30}	-0.5513	1.8592	1.3635	-1.7263	1.5186	1.1930	4.0550	2.0137	-1.7453	5.6001
	ω_{40}	1.2151	1.0537	1.0265	-0.7210	2.8249	0.7687	4.2906	2.0714	-2.8260	5.7902
250	ω_{10}	-1.1915	0.6926	0.8322	-1.7017	-0.7417	-1.2021	1.0008	1.0004	-2.1730	0.3156
	ω_{11}	1.0629	0.3692	0.6076	0.3214	1.8496	1.1965	1.8249	1.3509	-0.6821	3.9858
	ω_{20}	-0.9491	0.7488	0.8654	-1.9791	0.8249	-1.8104	5.4389	2.3322	-6.7399	0.8391
	ω_{21}	0.9071	0.0998	0.3160	0.2116	1.4994	0.9217	0.3404	0.5834	-0.2735	2.0725
	ω_{30}	-0.6196	1.8060	1.3439	-1.8731	0.8638	1.4677	4.5957	2.1438	-1.6677	5.9329
	ω_{40}	1.2863	1.0838	1.0410	-0.5338	3.0228	0.1857	4.6386	2.1537	-2.9124	5.2771

Table 3a. AE, MSE, RMSE and 95% CI for MLEs of TEOLLW QR model at $\tau = 0.75$ and CP = (0% and 30%)

n	Parameter	CP=0					CP=0.30				
		AE	MSE	RMSE	LCL	UCL	AE	MSE	RMSE	LCL	UCL
25	ω_{10}	-0.7500	0.8062	0.8979	-2.0582	0.4585	-0.7603	1.0110	1.0055	-2.1702	0.6854
	ω_{11}	0.4974	0.9889	0.9945	-1.3712	2.5120	0.5701	2.0552	1.4336	-1.8250	3.6169
	ω_{20}	-0.4300	2.2349	1.4949	-5.3893	2.0596	-0.8043	5.5960	2.3656	-6.6476	2.4387
	ω_{21}	0.4180	0.5800	0.7616	-0.8581	2.1449	0.3499	0.9995	0.9997	-1.5242	2.4649
	ω_{30}	0.0039	1.9459	1.3950	-1.5110	6.0794	0.3962	5.0954	2.2573	-1.9433	6.4192
	ω_{40}	0.5092	1.7479	1.3221	-1.4562	3.6184	0.8336	3.6921	1.9215	-1.3363	4.9421
100	ω_{10}	-0.7519	0.4911	0.7008	-1.2600	-0.2384	-0.7492	0.5237	0.7237	-1.3428	-0.0726
	ω_{11}	0.5165	0.2070	0.4550	-0.2475	1.2821	0.5110	0.3181	0.5640	-0.4158	1.5487
	ω_{20}	-0.5913	0.4673	0.6836	-1.2562	0.1707	-1.1006	3.4236	1.8503	-6.5055	1.3742
	ω_{21}	0.4199	0.0819	0.2863	-0.1373	1.0355	0.4352	0.1284	0.3583	-0.2602	1.1436
	ω_{30}	0.0601	0.6311	0.7944	-0.7760	1.3514	0.5184	3.8630	1.9654	-1.1666	6.4576
	ω_{40}	0.3441	0.4381	0.6619	-0.8801	1.5041	0.4339	0.9411	0.9701	-1.0103	2.4845
150	ω_{10}	-0.7351	0.4369	0.6610	-1.1119	-0.3961	-0.7353	0.4568	0.6758	-1.1745	-0.2504
	ω_{11}	0.5012	0.1245	0.3529	-0.0483	1.0612	0.4892	0.1819	0.4265	-0.3332	1.2397
	ω_{20}	-0.5883	0.3472	0.5892	-1.1524	-0.0952	-1.0557	2.7681	1.6638	-6.4704	0.6370
	ω_{21}	0.4173	0.0535	0.2313	-0.0512	0.8735	0.4215	0.0913	0.3022	-0.1274	1.0223
	ω_{30}	0.0783	0.5199	0.7210	-0.6119	1.1716	0.5415	3.3636	1.8340	-0.7574	6.5660
	ω_{40}	0.3006	0.3946	0.6282	-0.8356	1.4737	0.3222	0.6962	0.8344	-1.0202	1.8254
200	ω_{10}	-0.7413	0.4428	0.6655	-1.0876	-0.3977	-0.7420	0.4620	0.6797	-1.1706	-0.3022
	ω_{11}	0.5216	0.1266	0.3559	-0.0157	1.0907	0.5137	0.1820	0.4266	-0.1635	1.2984
	ω_{20}	-0.5380	0.1864	0.4317	-0.9657	-0.0287	-1.0446	2.8632	1.6921	-6.4718	0.3480
	ω_{21}	0.4053	0.0398	0.1994	0.0522	0.7793	0.4132	0.0719	0.2682	-0.1648	0.9164
	ω_{30}	0.0056	0.2723	0.5219	-0.6585	0.8451	0.5496	3.4788	1.8651	-0.6871	6.5573
	ω_{40}	0.3210	0.3293	0.5739	-0.6324	1.3858	0.2676	0.5577	0.7468	-0.9719	1.7402

n	Parameter	CP=0					CP=0.30				
		AE	MSE	RMSE	LCL	UCL	AE	MSE	RMSE	LCL	UCL
250	ω_{10}	-0.7266	0.4188	0.6471	-1.0877	-0.4160	-0.7348	0.4445	0.6667	-1.1519	-0.3204
	ω_{11}	0.4961	0.1018	0.3190	0.0176	1.0346	0.5064	0.1492	0.3863	-0.0868	1.1547
	ω_{20}	-0.5306	0.0978	0.3128	-0.9282	-0.1318	-1.1232	2.9263	1.7107	-6.4962	0.0625
	ω_{21}	0.3959	0.0328	0.1812	0.0636	0.7517	0.3919	0.0560	0.2366	-0.0869	0.8445
	ω_{30}	-0.0292	0.1518	0.3896	-0.6172	0.7909	0.6124	3.5755	1.8909	-0.6195	6.5333
	ω_{40}	0.3593	0.3422	0.5849	-0.6580	1.4721	0.2880	0.5113	0.7151	-0.8681	1.5627

Table 3b. AE, MSE, RMSE and 95% CI for MLEs of TEOLLW QR model at $\tau = 0.75$ and CP = (50% and 80%)

n	Parameter	CP=0.50					CP=0.80				
		AE	MSE	RMSE	LCL	UCL	AE	MSE	RMSE	LCL	UCL
25	ω_{10}	-0.8333	1.6038	1.2664	-2.5758	1.4958	-1.2755	4.3170	2.0777	-3.6830	2.8362
	ω_{11}	0.6588	4.2870	2.0705	-3.1543	4.7869	1.0090	15.6974	3.9620	-5.9732	11.0451
	ω_{20}	-1.0158	7.2206	2.6871	-6.4879	2.6786	-0.3816	4.3026	2.0743	-4.9339	2.8045
	ω_{21}	0.3928	1.3639	1.1678	-1.8781	2.5703	0.0129	4.2918	2.0717	-3.7470	3.6880
	ω_{30}	0.6352	7.0116	2.6479	-2.2929	6.2750	1.6480	9.3588	3.0592	-2.7199	5.9796
	ω_{40}	0.9894	5.1870	2.2775	-2.5910	5.5239	-0.1110	19.7238	4.4412	-6.2639	6.4693
100	ω_{10}	-0.7495	0.6471	0.8044	-1.5887	0.3615	-1.2082	2.4139	1.5537	-2.6601	1.6704
	ω_{11}	0.5410	0.6674	0.8169	-0.9328	2.1755	1.1521	5.9432	2.4379	-2.0775	6.3427
	ω_{20}	-1.3099	4.8314	2.1981	-6.5508	1.6600	-0.9727	3.6936	1.9219	-5.3799	1.8558
	ω_{21}	0.4271	0.2063	0.4542	-0.4674	1.2906	0.3380	0.7369	0.8584	-1.1859	2.0193
	ω_{30}	0.7646	5.1965	2.2796	-1.5368	6.4562	1.1430	6.4382	2.5374	-2.4750	5.6248
	ω_{40}	0.5619	2.1216	1.4566	-1.3835	4.0731	0.0431	6.0693	2.4636	-4.7755	5.1178
150	ω_{10}	-0.7092	0.4947	0.7033	-1.2982	-0.0103	-0.9027	1.9259	1.3878	-2.4256	1.8277
	ω_{11}	0.4484	0.3551	0.5959	-0.6987	1.6040	0.8891	4.3923	2.0958	-2.6561	6.2898
	ω_{20}	-1.0850	3.5330	1.8796	-6.5301	1.3681	-1.2509	3.9546	1.9886	-5.9128	1.3348
	ω_{21}	0.4524	0.1493	0.3864	-0.2562	1.1476	0.4199	0.4865	0.6975	-0.8537	1.8213

n	Parameter	CP=0.50					CP=0.80				
		AE	**MSE**	**RMSE**	**LCL**	**UCL**	**AE**	**MSE**	**RMSE**	**LCL**	**UCL**
	ω_{30}	0.5510	3.7021	1.9241	-1.3354	6.3217	1.2004	5.8149	2.4114	-2.1688	5.2346
	ω_{40}	0.3929	1.0771	1.0378	-1.0949	2.6627	0.2626	6.0140	2.4523	-3.4183	5.6186
200	ω_{10}	-0.7426	0.5035	0.7096	-1.3015	-0.1041	-0.7240	1.5900	1.2609	-2.1337	2.0821
	ω_{11}	0.5171	0.3046	0.5519	-0.4296	1.5871	0.8280	3.7790	1.9440	-2.4084	5.1631
	ω_{20}	-1.0655	3.5670	1.8887	-6.6099	1.4048	-1.4425	4.5985	2.1444	-6.1727	1.5155
	ω_{21}	0.4180	0.1058	0.3252	-0.2142	1.0889	0.3897	0.3900	0.6245	-0.7265	1.5712
	ω_{30}	0.5089	3.8265	1.9561	-1.3008	6.3905	1.0958	5.2975	2.3016	-2.1412	5.3475
	ω_{40}	0.3781	0.8453	0.9194	-0.9713	2.2167	0.5212	4.4785	2.1162	-3.2146	5.2944
250	ω_{10}	-0.7235	0.4709	0.6862	-1.2320	-0.0872	-0.7467	1.6093	1.2686	-2.2390	2.3139
	ω_{11}	0.4755	0.2650	0.5148	-0.4031	1.4544	0.7084	2.4689	1.5713	-2.4857	3.9841
	ω_{20}	-1.0093	2.8179	1.6787	-6.4940	1.3637	-1.3577	4.6227	2.1500	-5.9739	1.4904
	ω_{21}	0.4193	0.0928	0.3046	-0.2873	1.0124	0.3790	0.2518	0.5018	-0.6758	1.3253
	ω_{30}	0.4016	3.0583	1.7488	-1.1589	6.3849	1.1867	5.8420	2.4170	-2.0858	5.2212
	ω_{40}	0.4290	0.7553	0.8691	-0.8193	2.1125	0.2495	4.3929	2.0959	-3.3052	5.2040

5. Applications

The utilities of the new QR model are demonstrated using two datasets in this section. The first application considered censored gastric cancer data obtained from Kasurinen et al. (2018), and the second is uncensored or complete rent data, which are available in the R package, gamlss.data (Stasinopoulos et al., 2000). These datasets are chosen to justify the flexibility and robustness of the proposed QR in effectively capturing complex features, showcasing improved performance compared to existing models applied to these data. The Akaike Information Criteria (AIC) and Bayesian Information Criteria (BIC) are utilized to select the best model among the newly developed TEOLLW QR model and the existing candidate models considered in this study. The model with the lowest AIC and BIC values is deemed the optimum model. The quantiles, $\tau = 0.10,\ 0.25,\ 0.50,\ 0.75,$ and 0.99 are considered in the applications.

The study employed quantile residuals to diagnose the fitted models to assess the goodness of fit of the models. Specifically, index plots of the quantile residuals and probability (PP) plots are generated. The Kolmogorov-Smirnov (KS), Cramér-von Mises (CVM), and Anderson-Darling (AD) goodness-of-fit statistics, as well as their corresponding p-values, are presented as legends in the PP plots.

In addition to the EOLLW QR model (Rodrigues et al., 2023b), the performance of the TEOLLW QR model is compared with other existing models in the GAMLSS family, such as the normal (NO) regression models, lognormal 2 (LOGNO2), Weibull (WEI), Weibull type II (WEI2) and Weibull type III (WEI3). Their PDFs are presented in the Appendix.

The likelihood ratio (LR) test is used to compare the TEOLLW QR and its sub-models. The null hypothesis $H_0 : \xi_1 = \xi_1^*$ under the LR test is tested against the alternative hypothesis $H_1 : \xi_1 \neq \xi_1^*$. The test statistic is given by $\upsilon = 2\left\{\ell\left(\hat{\xi}\right) - \ell\left(\tilde{\xi}\right)\right\}$, where $\hat{\xi}$ are the estimates under the null hypothesis and $\tilde{\xi}$ are the estimates under the alternative hypothesis.

5.1 Data I: Gastric cancer data

Gastric cancer data is a survival dataset for patients suffering from gastric adenocarcinoma treated by surgery at Helsinki University Hospital in Finland (Kasurinen et al., 2018). It entails 301 persons with about 60% censored. The two covariates considered in this study are Lauren classification and the presence of distant metastasis. The structures of the variables are;

- t_i = Survival time measured in years,
- d_i = censoring indicator (1= observed and 0= censored),
- x_{1i} = Lauren classification (0= intestinal and 1= diffuse),
- x_{2i} = Presence of distant metastasis (0 = no, 1 = yes), where $i = 1, \ldots, 301$.

In this application, the censored MLE approach is employed since the data is censored. The two well-known information criteria (AIC and BIC) are employed to select the best-fit model among TEOLLW and its sub-models together with EOLLW (Rodrigues et al., 2023b). The results shown in Table 4 indicated that the proposed TEOLLW QR model is the best model for the data, since it has the lowest AIC and BIC values across the quantiles, with the exception of the BIC value at $\tau = 0.99$, where the TW sub-model obtained the lowest BIC score.

Table 4: AIC and BIC values of the fitted QR models for the gastric cancer data

τ		Models			
		TEOLLW	**TOLLW**	**TW**	**EOLLW**
0.10	AIC BIC	**745.3363** **774.9932**	757.7893 783.7390	789.6565 811.8992	750.3085 779.9654
0.25	AIC BIC	**743.8179** **773.4748**	757.7395 783.6893	89.6523 811.8949	750.1898 779.8499
0.50	AIC BIC	**743.6289** **773.2858**	757.6839 783.6337	789.6830 811.9257	750.1712 779.8281
0.75	AIC BIC	**743.6266** **773.2835**	757.6725 783.6222	89.7188 811.9615	750.1812 779.8381
0.99	AIC BIC	**786.4942** 816.1511	806.2778 832.2275	790.0397 **812.2823**	812.7450 842.4020

Bold means least values

Table 5 compares the TEOLLW QR model with its two sub-models, and the significant *p*-values support that the TEOLLW QR model provides a better fit to the data.

Table 5. LR test for the gastric cancer data

Models	**0.10**	**0.25**	**0.50**	**0.75**	**0.99**
TEOLLW vs. TOLLW	14.4530 (0.0001)	15.9217 (<0.0001)	16.0550 (<0.0001)	16.0458 (<0.0001)	21.78358 (<0.0001)
TEOLLW vs. TW	48.3202 (<0.0001)	49.8344 (<0.0001)	50.0541 (<0.0001)	50.0922 (<0.0001)	7.5455 (0.0230)

Table 6 presents the MLEs, standard errors (SEs) and *p*-values of the TEOLLW QR model using gastric data. The findings revealed that most estimates are significant at the 0.05 significance level.

Table 6a: MLEs, SEs and ***p***-values of TEOLLW QR for the gastric cancer data

τ	ξ	**MLEs**	**SEs**	***p*-value**
0.10	ϕ_{10}	0.3338	0.0471	<0.0001
	ϕ_{11}	0.2474	0.0627	<0.0001
	ϕ_{12}	-1.0772	0.1991	<0.0001
	ϕ_{20}	0.5048	0.0208	<0.0001
	ϕ_{21}	0.2474	0.0334	<0.0001
	ϕ_{22}	-0.5588	0.1041	<0.0001
	ϕ_{30}	1.3050	0.0150	<0.0001
	ϕ_{40}	-1.9475	0.0163	<0.0001
0.25	ϕ_{10}	1.1160	0.0482	<0.0001
	ϕ_{11}	0.5150	0.0632	<0.0001
	ϕ_{12}	-0.5719	0.1989	<0.0001
	ϕ_{20}	-0.0391	0.0321	<0.0001

τ	ξ	**MLEs**	**SEs**	***p*-value**
	ϕ_{21}	0.2546	0.0499	<0.0001
	ϕ_{22}	-0.5664	0.1623	<0.0001
	ϕ_{30}	1.8770	0.0224	<0.0001
	ϕ_{40}	-2.0233	0.0250	<0.0001
0.5	ϕ_{10}	2.0092	0.0483	<0.0001
	ϕ_{11}	0.3156	0.0632	<0.0001
	ϕ_{12}	0.0534	0.2020	0.792
	ϕ_{20}	-0.2102	0.0647	0.00129
	ϕ_{21}	0.2578	0.0836	0.00222
	ϕ_{22}	-0.5842	0.1370	<0.0001
	ϕ_{30}	2.0579	0.0370	<0.0001
	ϕ_{40}	-2.0505	0.0414	<0.0001
0.75	ϕ_{10}	2.3472	0.0483	<0.0001
	ϕ_{11}	0.2384	0.0632	0.0002
	ϕ_{12}	0.3040	0.2034	0.13613
	ϕ_{20}	-0.2081	0.0825	0.0122
	ϕ_{21}	0.2564	0.0958	0.00789
	ϕ_{22}	-0.5899	0.1140	<0.0001
	ϕ_{30}	2.0562	0.0381	<0.0001
	ϕ_{40}	-2.0500	0.0408	<0.0001

Table 6b: MLEs, SEs and ***p***-values of TEOLLW QR for the gastric cancer data

τ	ξ	**MLEs**	**SEs**	***p*-value**
0.99	ϕ_{10}	3.2439	0.1059	<0.0001
	ϕ_{11}	0.2296	0.1364	0.0933
	ϕ_{12}	3.3348	0.3078	<0.0001
	ϕ_{20}	0.0646	0.0425	0.1300
	ϕ_{21}	0.0767	0.0495	0.1220
	ϕ_{22}	-0.9528	0.0598	<0.0001
	ϕ_{30}	-0.7094	0.0675	<0.0001
	ϕ_{40}	1.0079	0.0409	<0.0001

Figure 2 presents the MLEs along with their respective 95% confidence intervals (CIs) plots, against quantiles in the range $[0.10, 0.99]$. These plots illustrate how variations in point estimates influence the response variable in different parts of the distribution. Estimates for ϕ_{10} and ϕ_{12} exhibit increasing trends in all quantiles, while ϕ_{11} displays a decreasing trend. Estimates for ϕ_{21} and ϕ_{22} demonstrate steady growth up to the 0.8^{th} quantile before decay, showing minor variations from the lower to the upper quantiles.

Estimates for ϕ_{30} and ϕ_{40} show minimal changes up to the 0.8^{th} quantile, however, as the quantile increases 0.99, ϕ_{30} declines sharply, and ϕ_{40} rises considerably. Meanwhile, the estimate ϕ_{20} displays a U-shaped trend, suggesting a nonlinear effect with a stronger influence at the extreme quantiles. Although most of the effects appear statistically significant, the CIs for ϕ_{20}, ϕ_{22}, ϕ_{30}, and ϕ_{40} cross zero at certain quantiles indicate a lack of significant effects in these areas.

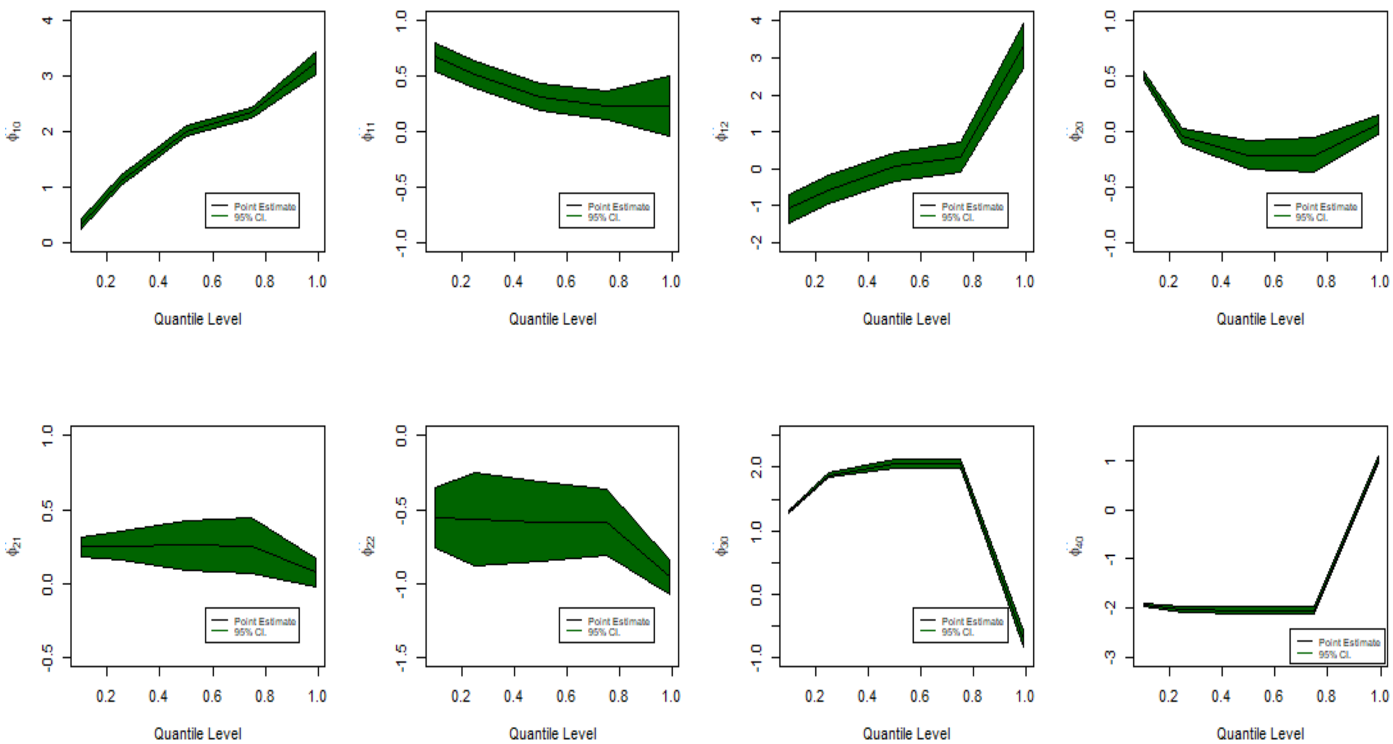

Figure 2: Point estimates and 95% CIs by quantiles for gastric cancer data

Figure 3 presents the index plots of the quantile residuals for the TEOLLW QR model. The results indicate the adequacy of the model because most of the points are spread uniformly around zero and are within the interval $[-3,3]$.

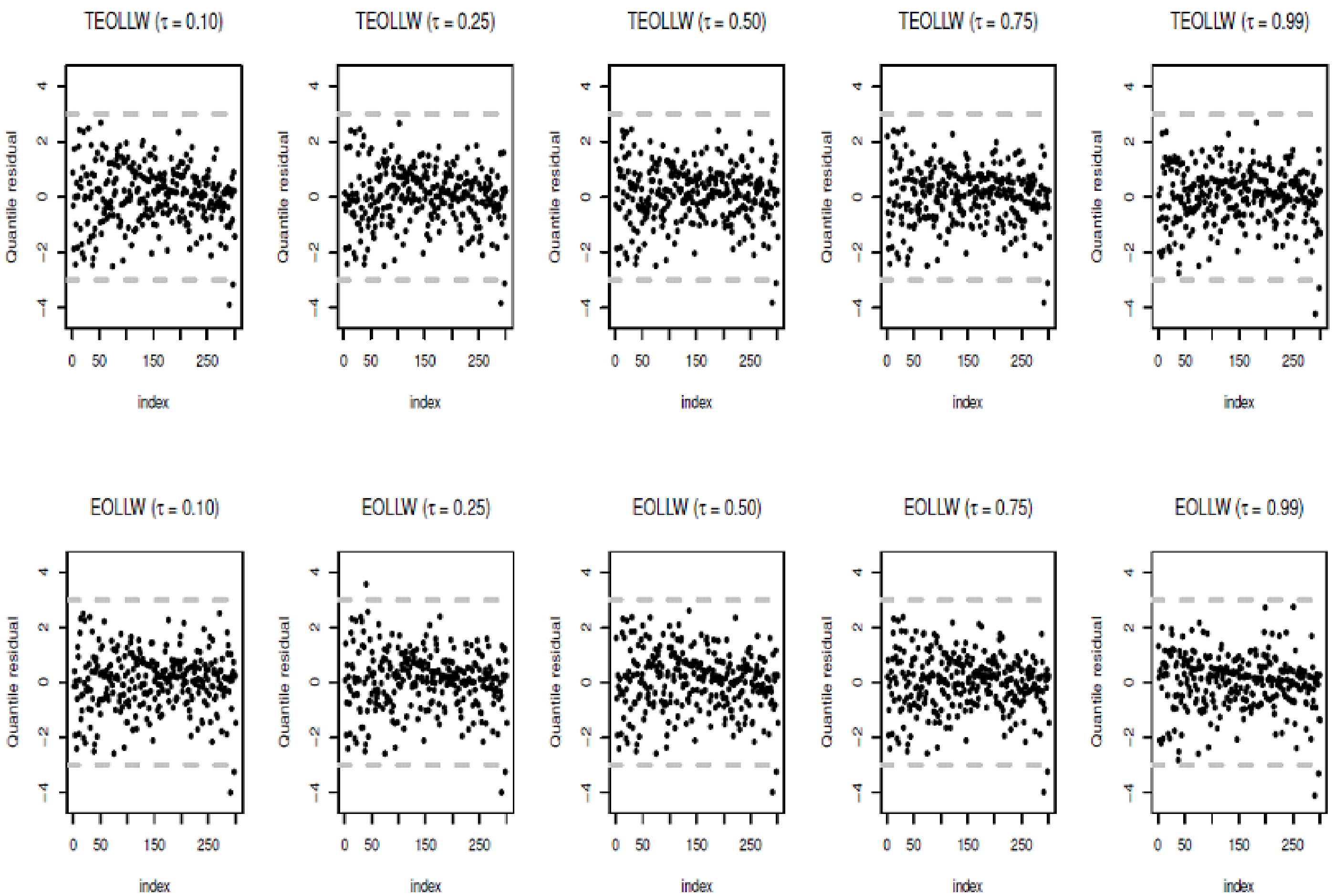

Figure 3. Index plots of quantile residuals for gastric cancer data

Figure 4 shows the PP plots of the quantile residuals. The results indicated that, except for the 0.99 quantile, the points closely mimic the diagonal line. In addition, KS, CVM and AD have smaller test statistics values with corresponding higher *p*-values (greater than the 0.05 significance level) compared to those of the candidate models. Hence, the newly proposed model shows superior performance and can serve as an alternative to some existing models.

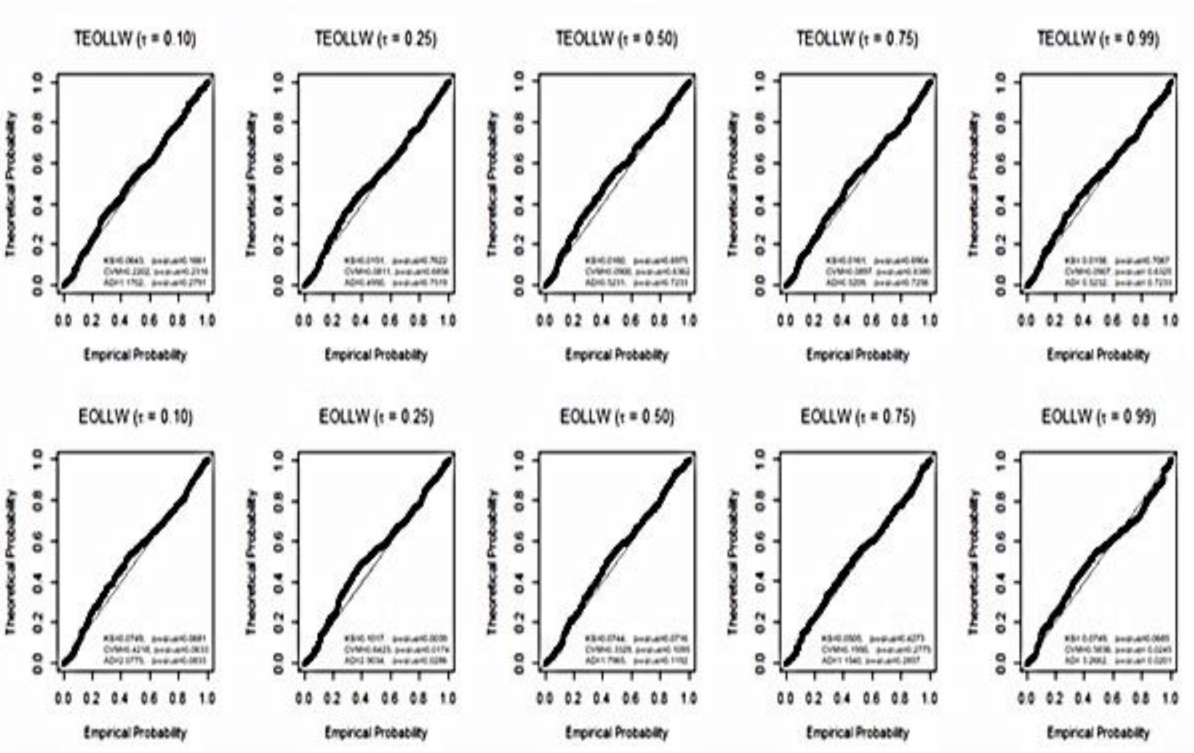

Figure 4. Quantile residuals' PP-plot for gastric cancer data

The MLEs, SEs (in parenthesis), *p*-values (beneath SEs), AIC, and BIC values of the candidate mean regression models are presented in Table 7. The results reveal that the AICs and BICs for these models are higher than those of the TEOLLW QR model, indicating that the TEOLLW QR model performs better for gastric cancer data.

Table 7: MLEs, SEs, ***p***-values, AIC and BIC of mean regression models for gastric cancer data

Model	$\hat{\phi}_{10}$	$\hat{\phi}_{11}$	$\hat{\phi}_{12}$	$\hat{\phi}_{20}$	$\hat{\phi}_{21}$	$\hat{\phi}_{22}$	AIC	BIC
	7.7447	2.3436	-1.5818	1.4490	0.0549	0.0142		
NO	(0.4056)	(0.5177)	(0.6393)	(0.0671)	(0.0838)	(0.1012)	789.223	811.47
	<0.0001	<0.0001	0.0139	<0.0001	0.5130	0.8890		
	1.7548	0.5578	1.8946	0.2103	0.1550	0.9135		
LOGNO2	(0.1229)	(0.1706)	(0.4416)	(0.0671)	(0.0838)	(0.1012)	900.99	923.23
	<0.0001	0.0012	<0.0001	0.0019	0.0654	<0.0001		
	2.1242	0.3060	1.3511	0.3778	0.1488	-1.0379		
WEI	(0.0683)	(0.0839)	(0.2244)	(0.0703)	(0.0878)	(0.1060)	797.49	819.73
	<0.0001	0.0003	<0.0001	<0.0001	0.0910	<0.0001		
	-3.1757	-0.7990	1.5239	0.3975	0.0971	-1.0426		
WEI2	(0.0949)	(0.1185)	(0.1431)	(0.0256)	(0.0308)	(0.0458)	798.10	820.35
	<0.0001	<0.0001	<0.0001	<0.0001	0.0018	<0.0001		
	2.0255	0.2912	1.9446	0.3839	0.1364	-1.0330		
WEI3	(0.0679)	(0.0838)	(0.2241)	(0.0725)	(0.0900)	(0.1070)	797.57	819.81
	<0.0001	0.0006	<0.0001	<0.0001	0.1310	<0.0001		

5.2 Data II: Rent Data

The rent data from the GAMLSS package is used for the second application. The datasets were obtained from a survey of accommodation in Munich. The data consists of nine variables with 1,969 observations. This study considered variables: The dependent variable, net rent in Deutsche Mark (R), and one covariate, floor space in square meters (Fl).

The TEOLLW QR model is compared to TOLLW, TW, and EOLLW QR models using AIC and BIC. The findings in Table 8 revealed that the TEOLLW QR model is better than the competing models for the rent data, as it has the lowest values of AIC and BIC.

Table 8. AIC and BIC values of the fitted QR models for the rent data

τ		Models			
		TEOLLW	**TOLLW**	**TW**	**EOLLW**
0.10	AIC BIC	**28083.1600** **28116.6700**	28091.8600 28119.7900	28145.6000 28167.9400	28106.5200 28140.0300
0.25	AIC BIC	**28083.1600** **28116.6700**	28090.3600 28118.2800	28145.3100 28167.6600	28093.7000 28127.2100
0.50	AIC BIC	**28082.7600** **28116.2700**	28088.9000 28116.8300	28144.8700 28167.2100	28086.9500 28120.4600
0.75	AIC BIC	**28082.5900** **28116.1000**	28084.7800 28118.2900	28144.5900 28166.9300	28087.5600 28121.0700
0.99	AIC BIC	**28082.2500** **28115.7600**	28088.1000 28116.0200	28145.0000 28167.3400	28095.7800 28129.2900

Bold means least value

In parametric regression using rent data, the LR test was performed to compare TEOLLW and submodels. The results displayed in Table 9 revealed that the TEOLLW QR model is the most suitable for the data.

Table 9. LR test for rent data

Models	**0.10**	**0.25**	**0.50**	**0.75**	**0.99**
TEOLLW vs. TOLLW	10.7012	9.1994	8.1446	28.8367	7.8463
	(0.0011)	(0.0024)	(0.0043)	(<0.0001)	(0.0051)
TEOLLW vs. TW	66.4367	66.1581	66.1089	66.0031	66.7496
	(<0.0001)	(<0.0001)	(<0.0001)	(<0.0001)	(<0.0001)

Table 10 presents the parameter estimates, SEs, and *p*-values of the TEOLLW QR model at the various quantiles are presented. The parameter estimates are significant, as their *p*-values are far lower than the 0.05 significance level.

Figure 5 displays the plots of the estimates with their corresponding CIs against quantiles in the range $[0.10, 0.99]$. Estimates for ϕ_{10} and ϕ_{11} show a progressive and stronger influence as they move toward higher quantiles. The rest show constant growth, which is an indication that there are no variations in their effects. The magnitude of their effects is statistically significant since the CIs do not include zero.

Table 10. MLEs, SEs and *p*-values of TEOLLW QR for the rent data

τ	ξ	**MLEs**	**SEs**	***p*-value**
0.1	ϕ_{10}	5.4183	0.0315	<0.0001
	ϕ_{11}	0.0089	0.0005	<0.0001
	ϕ_{20}	0.7338	0.0345	<0.0001
	ϕ_{21}	-0.0024	0.0005	<0.0001
	ϕ_{30}	0.1755	0.0115	<0.0001
	ϕ_{40}	0.5755	0.0192	<0.0001
0.25	ϕ_{10}	5.6161	0.0316	<0.0001
	ϕ_{11}	0.0095	0.0005	<0.0001
	ϕ_{20}	0.7372	0.0435	<0.0001
	ϕ_{21}	-0.0025	0.0006	<0.0001
	ϕ_{30}	0.2234	0.0152	<0.0001
	ϕ_{40}	0.5002	0.0265	<0.0001
0.5	ϕ_{10}	5.9339	0.0314	<0.0001
	ϕ_{11}	0.0104	0.0005	<0.0001
	ϕ_{20}	0.7421	0.0589	<0.0001
	ϕ_{21}	-0.0025	0.0008	<0.0001
	ϕ_{30}	0.1690	0.0231	<0.0001
	ϕ_{40}	0.5843	0.0374	<0.0001
0.75	ϕ_{10}	6.1459	0.0314	<0.0001
	ϕ_{11}	0.0111	0.0005	<0.0001
	ϕ_{20}	0.7458	0.0600	<0.0001
	ϕ_{21}	-0.0026	0.0009	<0.0001
	ϕ_{30}	0.1692	0.0230	<0.0001
	ϕ_{40}	0.5833	0.0378	<0.0001
0.99	ϕ_{10}	6.5568	0.0314	<0.0001
	ϕ_{11}	0.0124	0.0005	<0.0001
	ϕ_{20}	0.7480	0.0398	<0.0001
	ϕ_{21}	-0.0027	0.0006	<0.0001
	ϕ_{30}	0.1513	0.0212	<0.0001
	ϕ_{40}	0.6180	0.0311	<0.0001

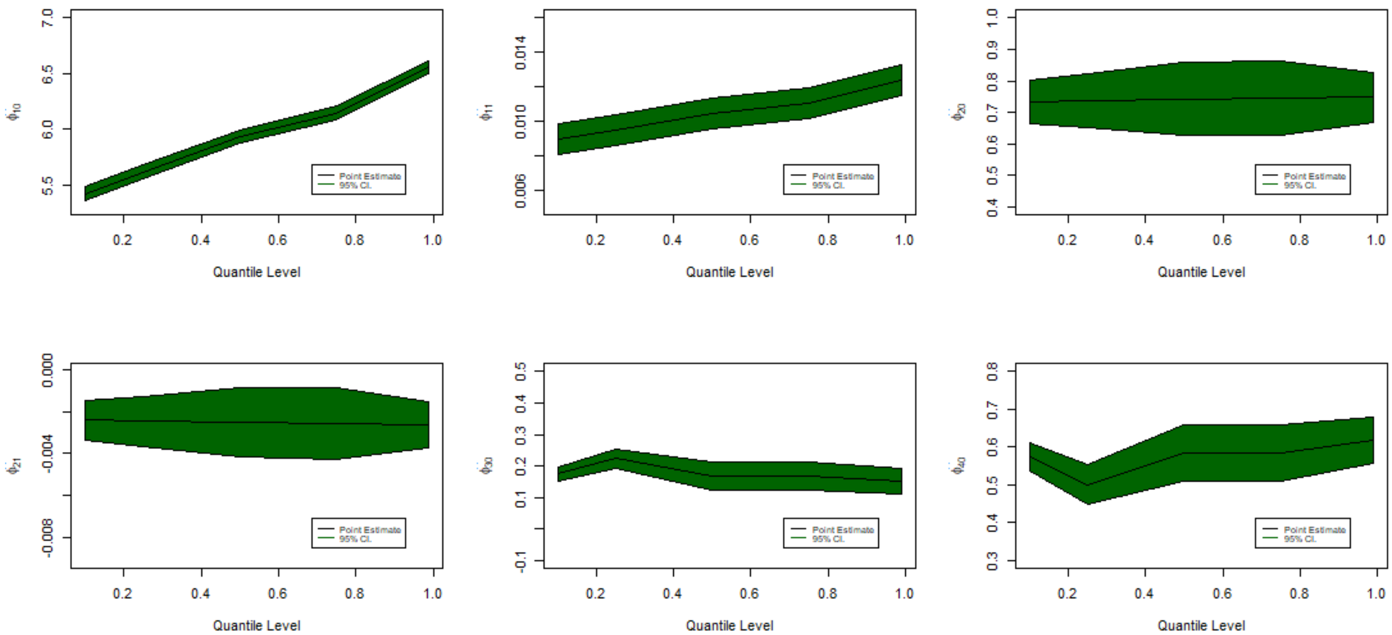

Figure 5. Point estimates and 95% CIs by quantiles for rent data

The index plots of the quantile residuals are shown in Figure 6. These plots demonstrate that the models perform well with the rent data, as the residuals fall randomly around zero within the range [−3, 3].The random distribution of the residuals points to the fact that there are no obvious patterns in the residuals, suggesting a good fit of the model with the rent data.

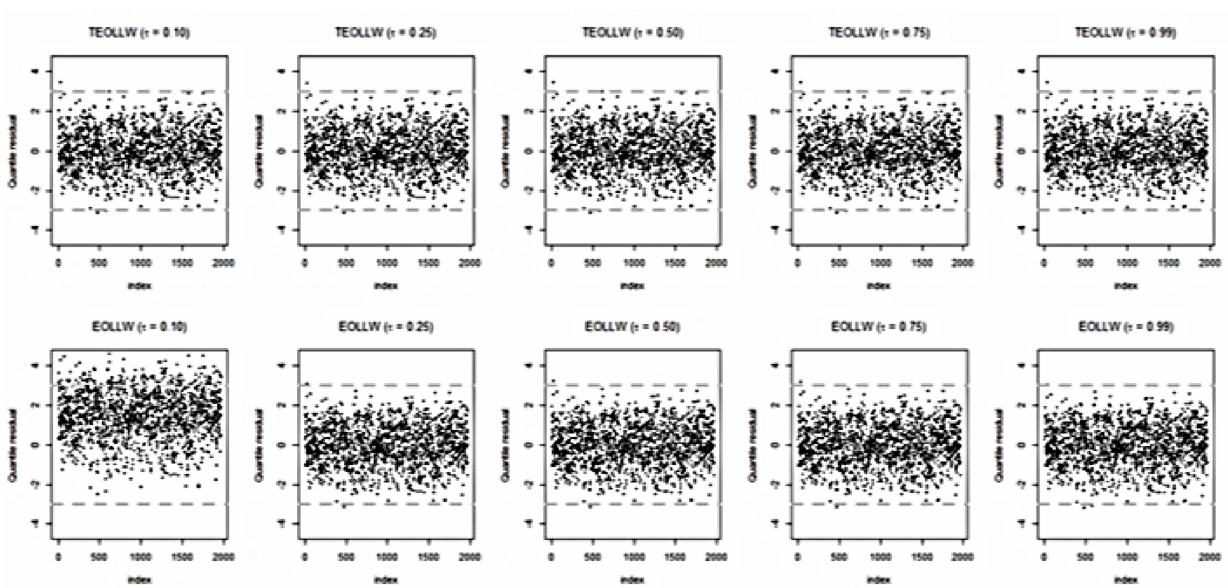

Figure 6. Index plots of quantile residuals for rent data

PP plots and goodness-of-fit tests are shown in Figure 7. They revealed that the TEOLLW QR model best fits the rent data.

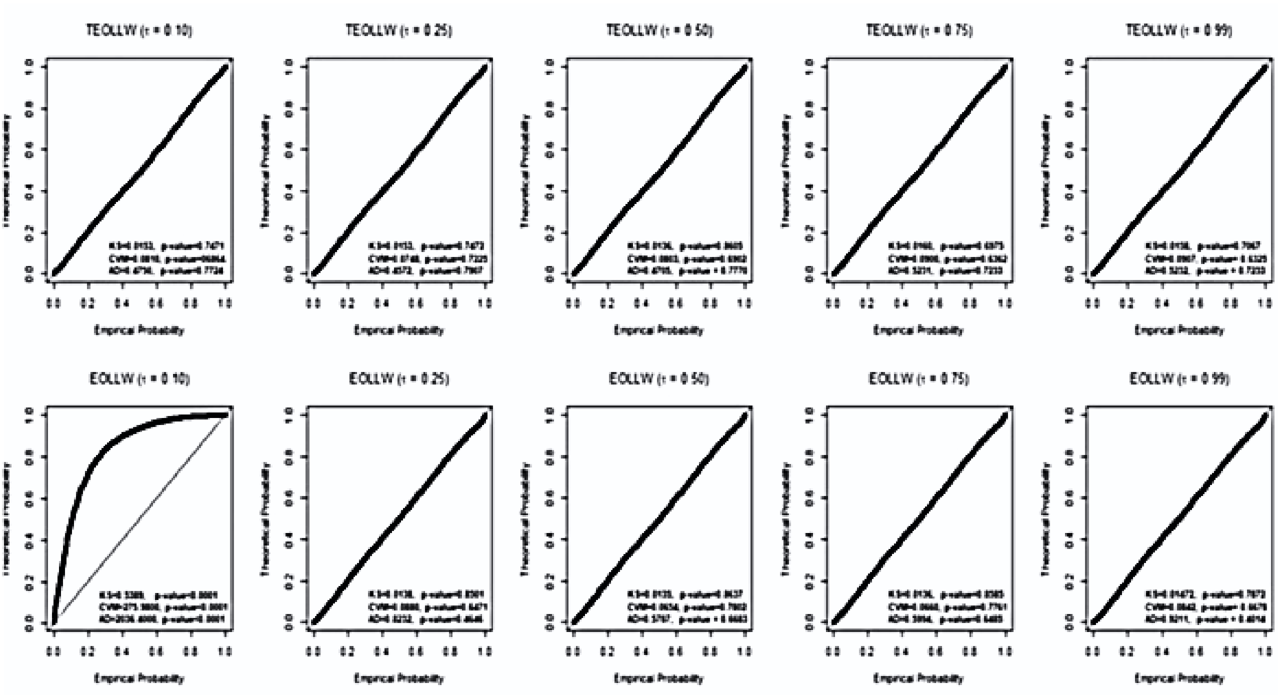

Figure 7. Quantile residuals' PP-plot for rent data

Table 11 gives the MLEs, SEs (in parentheses), *p*-values (beneath SEs), AIC, and BIC of the candidate models from the GAMLSS family. The results indicated that the new QR model performs better.

Table 11. MLEs, SEs, ***p***-values, AIC and BIC of mean regression models for the rent data

Model	$\hat{\phi}_{10}$	$\hat{\phi}_{11}$	$\hat{\phi}_{20}$	$\hat{\phi}_{21}$	AIC	BIC
NO	251.4070	8.2420	4.8543	0.0131	28197.21	28219.55
	21.0680	0.3490	0.0542	0.0008		
	<0.0001	<0.0001	<0.0001	<0.0001		
LOGNO2	5.8950	0.0103	-0.9779	0.0020	28222.19	28244.53
	0.0324	0.0005	0.0542	0.0008		
	<0.0001	<0.0001	<0.0001	0.0102		
WEI	6.0595	0.0108	1.1866	-0.0027	28088.76	28144.62
	0.0275	0.0004	0.0567	0.0008		
	<0.0001	<0.0001	<0.0001	0.0008		
WEI2	-16.3410	-0.0269	0.9949	-0.0002	28123.15	28145.49
	0.0766	0.0011	0.0042	0.0001		
	<0.0001	<0.0001	<0.0001	0.0068		
WEI3	5.9494	0.0107	1.1887	-0.0027	28112.62	28134.96
	0.0275	0.0004	0.0552	0.0008		
	<0.0001	<0.0001	<0.0001	0.0006		

6. Conclusion

This study introduces a novel quantile regression model tailored for censored and uncensored data, grounded in the proposed distribution. The maximum likelihood method was employed to estimate the parameters of the proposed quantile regression model, and the consistency of the estimation method was evaluated through a Monte Carlo simulation study. The practical utility of the model was demonstrated using gastric cancer and rental price datasets. The results indicate that the new quantile regression model provides a better fit than the exponentiated odd log-logistic quantile regression and several existing models within the GAMLSS framework. Future work will aim to extend the applicability of this model by incorporating a semiparametric approach, which can more explicitly capture nonlinear effects and potentially yield more robust results.

Funding: *The authors declare that no funding was received for this research.*

Conflict of Interest: *The authors declare that they have no conflict of interest.*

References

Abd EL-Baset, A. A. and Ghazal, M. G. (2020). Exponentiated additive Weibull distribution. *Reliability Engineering & System Safety*, 193:106663. http://doi.org/10.1016/j.ress.2019.106663.

Abubakari, A. G., Luguterah, A., and Nasiru, S. (2022). Unit exponentiated fréchet distribution: Actuarial measures, quantile regression and applications. *Journal of the Indian Society for Probability and Statistics*, 23(2):387–424. http://doi.org/10.1007/s41096-022-00129-2.

Ahmad, Z. and Iqbal, B. (2017). Generalized flexible Weibull extension distribution. *Circulation in Computer Sciences*, 2(4):68–75. https://doi.org/10.22632/ccs-2017-252-11.

Alghamdi, S. M., Albalawi, O., Almarzouki, S. M., Nagarjuna, V. B., Nasiru, S., and Elgarhy, M. (2024). Different estimation methods of the modified kies topp-leone model with applications and quantile regression. *PLOS ONE*, 19(9):e0307391. https://doi.org/10.1371/journal.pone.0307391.

Alizadeh, M., Tahmasebi, S., and Haghbin, H. (2020). The exponentiated odd log-logistic family of distributions: Properties and applications. *Journal of Statistical Modelling: Theory and Applications*, 1(1):29–52. https://doi.org/10.22034/jsmta.2020.1707.

Cordeiro, G. M., Biazatti, E. C., and de Santana, L. H. (2023). A new extended Weibull distribution with application to influenza and hepatitis data. *Stats*, 6(2):657–673. https://doi.org/10.3390/stats6020042.

Cruz, J. N. D., Ortega, E. M., and Cordeiro, G. M. (2016). The log-odd log-logistic Weibull regression model: modelling, estimation, influence diagnostics and residual analysis. *Journal of Statistical Computation and Simulation*, 86(8):1516–1538. https://doi.org/10.1080/00949655.2015.1069623.

de Araújo, F. J. M., Guerra, R. R., and Peña-Ramírez, F. A. (2022). The Burr XII quantile regression for salary-performance models with applications in the sports economy. *Computational and Applied Mathematics*, 41(6):282. https://doi.org/10.1007/s40314-022-01810-5.

Dunn, P. K. and Smyth, G. K. (1996). Randomized quantile residuals. *Journal of Computational and Graphical Statistics*, 5(3):236–244. https://doi.org/10.2307/1390802.

Galton, F. (1886). Regression towards mediocrity in hereditary stature. *The Journal of the Anthropological Institute of Great Britain and Ireland*, 15:246–263. https://doi.org/10.2307/2841583.

Ghazal, M. G. M. (2023). A new extension of the modified Weibull distribution with applications for engineering data. *Probabilistic Engineering Mechanics*, 74:103523. https://doi.org/10.1016/j.probengmech.2023.103523.

Hastie, T. and Tibshirani, R. (1986). Generalized additive models. *Statistical Science*, 1(4):297–310. https://doi.org/10.1214/ss/1177013604.

Huang, Q., Zhang, H., Chen, J., and He, M. (2017). Quantile regression models and their applications: A review. *Journal of Biometrics & Biostatistics*, 8(3):1–6. https://doi.org/10.4172/2155-6180.1000362.

Ishaq, A. I. and Abiodun, A. A. (2020). The maxwell–Weibull distribution in modeling lifetime datasets. *Annals of Data Science*, 7(4):639–662. https://doi.org/10.1007/s40745-020-00288-8.

Jiang, D., Han, Y., Cui, W., Wan, F., Yu, T., and Song, B. (2023). An improved modified Weibull distribution applied to predict the reliability evolution of an aircraft lock mechanism. *Probabilistic Engineering Mechanics*, 72:103449. https://doi.org/10.1016/j.probengmech.2023.103449.

Kasurinen, A., Tervahartiala, T., Laitinen, A., Kokkola, A., Sorsa, T., B¨ockelman, C., and Haglund, C. (2018). High serum mmp-14 predicts worse survival in gastric cancer. *PLOS ONE*, 13(12):1-11. https://doi.org/10.1371/journal.pone.0209549.

Koenker, R. and Bassett, G. (1978). Regression quantiles. *Econometrica*, 46:33–50. https://doi.org/10.2307/1913643.

Korkmaz, M. C., Altun, E., Chesneau, C., and Yousof, H. M. (2022). On the unit-chen distribution with associated quantile regression and applications. *Mathematica Slovaca*, 72(3):765–786. https://doi.org/10.1515/ms-2022-0092.

Korkmaz, M. , Chesneau, C., and Korkmaz, Z. S. (2021). On the arcsecant hyperbolic normal distribution. properties, quantile regression modeling and applications. *Symmetry*, 13(1):117. https://doi.org/10.3390/sym13010117.

Mazucheli, J., Alves, B., Korkmaz, M. , and Leiva, V. (2022). Vasicek quantile and mean regression models for bounded data: New formulation, mathematical derivations, and numerical applications. *Mathematics*, 10(9):1389. https://doi.org/10.3390/math10091389.

Mazucheli, J., Korkmaz, M. C¸., Menezes, A. F., and Leiva, V. (2023). The unit generalized half-normal quantile regression model: formulation, estimation, diagnostics, and numerical applications. *Soft Computing*, 27(1):279–295. https://doi.org/10.1007/s00500-022-06914-5.

Mazucheli, J., Leiva, V., Alves, B., and Menezes, A. F. (2021). A new quantile regression for modeling bounded data under a unit birnbaum–saunders distribution with applications in medicine and politics. *Symmetry*, 13(4):682. https://doi.org/10.3390/sym13040682.

Mazucheli, J., Menezes, A. F. B., Fernandes, L. B., Oliveira, R. P., and Ghitany, M. E. (2020). The unit-Weibull distribution as an alternative to the kumaraswamy distribution for the modelling of quantiles conditional on covariates. *Journal of Applied Statistics*, 47:954–974. https://doi.org/10.1080/02664763.2019.1637694.

Muhammad, M., Abba, B., Xiao, J., Alsadat, N., Jamal, F., and Elgarhy, M. (2024). A new three-parameter flexible unit distribution and its quantile regression model. *IEEE Access*, 12:156235–156251. https://doi.org/10.1109/ACCESS.2024.3374898.

Mustapha, M., H., B., and Nasiru, S. (2022). Unit gamma/gompertz quantile regression with applications to skewed data. *Sri Lankan Journal of Applied Statistics*, 23(1):49–73. 10.4038/sljastats.v23i1.8089.

Nasiru, S., Abubakari, A. G., and Chesneau, C. (2023). The arctan power distribution: Properties, quantile and modal regressions with applications to biomedical data. *Mathematical and Computational Applications*, 28(1):25. https://doi.org/10.3390/mca28010025.

Nasiru, S. and Chesneau, C. (2023). Developments of efficient trigonometric quantile regression models for bounded response data. *Axioms*, 12(4):350. 10.3390/axioms12040350.

Nassar, M., Afify, A. Z., Dey, S., and Kumar, D. (2018). A new extension of Weibull distribution: properties and different methods of estimation. *Journal of Computational and Applied Mathematics*, 336:439–457. https://doi.org/10.1016/j.cam.2017.12.001

Nelder, J. A. and Wedderburn, R. W. (1972). Generalized linear models. *Journal of the Royal Statistical Society Series A: Statistics in Society*, 135(3):370–384. https://doi.org/10.2307/2344614.

Noufaily, A. and Jones, M. (2013). Parametric quantile regression based on the generalized gamma distribution. *Journal of the Royal Statistical Society. Series C (Applied Statistics)*, 62:723–740. https://doi.org/10.1111/rssc.12014.

Ortega, E. M., Cordeiro, G. M., and Kattan, M. W. (2013). The log-beta Weibull regression model with application to predict recurrence of prostate cancer. *Statistical Papers*, 54(1):113– 132. https:/doi.org/10.1007/s00362-011-0414-1

Peng, X. and Yan, Z. (2014). Estimation and application for a new extended Weibull distribution. *Reliability Engineering and System Safety*, 121:34–42. https://doi.org/10.1016/j.ress.2013.07.007.

Prataviera, F., Silva, A. M., Cardoso, E. J., Cordeiro, G. M., and Ortega, E. M. (2021). A novel generalized odd log-logistic maxwell-based regression with application to microbiology. *Applied Mathematical Modelling*, 93:148–164. https://doi.org/10.1016/j.apm.2020.12.003.

Ribeiro, T. F., Peña-Ramírez, F. A., Guerra, R. R., and Cordeiro, G. M. (2022). Another unit Burr XII quantile regression model based on the different reparameterization applied to dropout in brazilian undergraduate courses. *PLOS ONE*, 17(11):e0276695. https://doi.org/10.1371/journal.pone.0276695.

Rigby, R. A. and Stasinopoulos, D. M. (2005). Generalized additive models for location, scale and shape. *Journal of the Royal Statistical Society Series C: Applied Statistics*, 54(3):507–554. https://doi.org/10.1111/j.1467-9876.2005.00510.x.

Rodrigues, G. M., Ortega, E. M., and Cordeiro, G. M. (2023a). New partially linear regression and machine learning models applied to agronomic data. *Axioms*, 12(11):1027. 10.3390/axioms12111027.

Rodrigues, G. M., Ortega, E. M., Cordeiro, G. M., and Vila, R. (2022). An extended Weibull regression for censored data: Application for covid-19 in campinas, brazil. *Mathematics*, 10(19):3644. https://doi.org/10.3390/math10193644.

Rodrigues, G. M., Ortega, E. M., Cordeiro, G. M., and Vila, R. (2023b). Quantile regression with a new exponentiated odd log-logistic Weibull distribution. *Mathematics*, 11(6):1518. 10.3390/math11061518.

Rodrigues, G. M., Ortega, E. M. M., Vila, R., and Cordeiro, G. M. (2023c). A new extended normal quantile regression model: properties and applications. *Communications in Statistics– Simulation and Computation*, pages 1–22. 10.1080/03610918.2023.2193218.

Sánchez, L., Leiva, V., Saulo, H., Marchant, C., and Sarabia, J. M. (2021). A new quantile regression model and its diagnostic analytics for a Weibull distributed response with applications. *Mathematics*, 9(21):2768. 10.3390/math9212768.

Sarhan, A. M. and Apaloo, J. (2013). Exponentiated modified Weibull extension distribution. *Reliability Engineering & System Safety*, 112:137–144. https://doi.org/10.1016/j.ress.2012.10.013.

Shakhatreh, M. K., Lemonte, A. J., and Moreno-Arenas, G. (2019). The log-normal modified Weibull distribution and its reliability implications. *Reliability Engineering & System Safety*, 188:6–22. https://doi.org/10.1016/j.ress.2019.03.014.

Souza, L., Júnior, W. R. D. O., Brito, C. C. R. D., Chesneau, C., Fernandes, R. L., and Ferreira, T. A. (2021). Tan-g class of trigonometric distributions and its applications. *Cubo (Temuco)*, 23(1):1–20. http://dx.doi.org/10.4067/S0719-06462021000100001.

Stasinopoulos, D. M., Rigby, R. A., and Fahrmeir, L. (2000). Modelling rental guide data using mean and dispersion additive models. *Journal of the Royal Statistical Society: Series D (The Statistician)*, 49(4):479–493. https://doi.org/10.1111/1467-9884.00247.

Stasinopoulos, M. D., Rigby, R. A., Heller, G. Z., Voudouris, V., and De Bastiani, F. (2017). *Flexible regression and smoothing: using GAMLSS in R*. CRC Press. https://doi.org/10.18637/jss.v085.b02.

Suleiman, A. A., Daud, H., Ishaq, A. I., Kayid, M., Sokkalingam, R., Hamed, Y., and Elgarhy, M. (2024). A new Weibull distribution for modeling complex biomedical data. *Journal of Radiation Research and Applied Sciences*, 17(4):101190. https://doi.org/10.1016/j.jrras.2024.101190.

Appendix

The competing models except the EOLLW QR model can be accessed in R package by loading **library(gamlss.dist)**. Their PDFs are provided below;

- EOLLW QR model:

$$f(z)=\frac{\gamma\lambda\sigma z^{\sigma-1}\eta\varpi^{\gamma}\left(1-\varpi\right)^{\gamma\lambda-1}}{\rho^{\sigma}\left\{\left(1-\varpi\right)^{\gamma}+\varpi^{\gamma}\right\}^{\lambda+1}},z>0,$$

where $\eta=-\log\left\{\frac{\left(1-\tau^{\frac{1}{\lambda}}\right)^{\frac{1}{\gamma}}}{\left[\tau^{\frac{1}{\gamma\lambda}}+\left(1-\tau^{\frac{1}{\lambda}}\right)^{\frac{1}{\gamma}}\right]}\right\}$, $\varpi=\exp\left[-\eta\left(\frac{z}{\rho}\right)^{\sigma}\right]$, $\gamma>0,\ \lambda>0,\ \rho>0,\ \sigma>0$ and $\tau\in\left(0,1\right)$ is fixed.

- NO distribution

$$f\left(z\right)=\frac{1}{\sqrt{2\pi\sigma^{2}}}e^{-\frac{\left(z-\mu\right)^{2}}{2\sigma^{2}}},\ -\infty<z<\infty,\ \sigma>0,\ \mu\in\left(-\infty,+\infty\right),$$

where μ is the mean and σ is the standard deviation.

- LOGNO2$\left(\mu;\sigma\right)$

$$f\left(z\right)=\frac{1}{z\sigma\sqrt{2\pi}}e^{-\frac{\left(\ln(z)-\ln\left(\mu\right)\right)^{2}}{2\sigma^{2}}},\ z>0,\ \sigma>0,\ \mu>0,$$

where μ is the median and σ is the standard deviation.

- WEI distribution

$$f(z)=\frac{\sigma z^{\sigma-1}}{\rho^{\sigma}}e^{-\left(\frac{z}{\rho}\right)^{\sigma}},\ z>0,\rho>0\ ,\sigma>0.\ .$$

- WEI2 distribution

$$f(z)=\sigma\rho z^{\sigma-1}e^{-\rho\sigma z},\ z>0,\rho>0\ ,\sigma>0.$$

- WEI3 distribution

$$f(z)=\frac{\sigma}{\delta}\left(\frac{z}{\delta}\right)^{\sigma-1}e^{-\left(\frac{z}{\delta}\right)^{\sigma}},\ z>0,$$

where $\delta=\frac{\rho}{\Gamma\left((1/\sigma)+1\right)}$, $\rho>0$ and $\sigma>0.$

Acronyms

AIC	Akaike Information Criteria
BIC	Bayesian Information Criteria
CDF	Cumulative Distribution Function
CP	Coverage Percentage
CI	Confidence Interval
CVM	Cramér-von Mises
EOLL-G	Exponentiated Odd Log-Logistic
EOLLW	Exponent1ated Odd Log-Logistic Weibull
GAM	Generalized Additive Model
GAMLSS	Generalized Additive Model for Location, Shape and Scale
GLM	Generalized Linear Model
HRF	Hazard Rate Function
KS	Kolmogorov-Smirnov
LM	Linear Model
LR	Likelihood Ratio
MLE	Maximum Likelihood Estimation
MLEs	Maximum Likelihood Estimators
MSE	Mean Square Error
PDF	Probability Density Function
QR	Quantile Regression
RMSE	Root Mean Square Error
SF	Survival Function
SEs	Standard Errors
tan	Tangent
TEOLL	Tan Exponentiatel Odd Log-Logistic
TEOLLW	Tan Exponentiatel Odd Log-Logistic Weibull
WEI	Weibull
WEI2	Weibull II
WEI3	Weibull III